

Physikalisch- Technische Bundesanstalt




DKD

Guide Procedures for a traceable DKD-L 02-2 RF voltage measurement

Edition 04/2014

<https://doi.org/10.7795/550.20190509>



	<p>Procedures for a traceable RF voltage measurement</p> <p>https://doi.org/10.7795/550.20190509</p>	DKD-L 02-2	
		Edition:	04/2014
		Revision:	0
		Page:	2 / 47

Deutscher Kalibrierdienst (DKD)


Since its foundation in 1977, the DKD brought together calibration laboratories of industrial enterprises, research institutes, technical authorities, inspection and testing institutes. On 3 May 2011, the DKD was reestablished as a *technical body* of the PTB and the accredited laboratories.

This body is called *Deutscher Kalibrierdienst (DKD – German Calibration Service)* and is under the direction of the PTB. The guidelines and guides elaborated by the DKD represent the state of the art in the respective technical areas of expertise and can be used by the *Deutsche Akkreditierungsstelle GmbH* (the German accreditation body – DAkkS) for the accreditation of calibration laboratories.

The accredited calibration laboratories are now accredited and monitored by the DAkkS as legal successor of the DKD. They carry out calibrations of measuring devices and measuring standards for the measured values and measuring ranges defined during accreditation. The calibration certificates issued by these laboratories prove the traceability to national standards as required by the family of standards DIN EN ISO 9000 and DIN EN ISO/IEC 17025.

Contact:

Physikalisch-Technische Bundesanstalt (PTB)
 DKD Executive Office
 Bundesallee 100 38116 Braunschweig
 P.O. Box 33 45 38023 Braunschweig
 Telephone Office: 0049 531 5 92-8021
 Internet: www.dkd.eu

	Procedures for a traceable RF voltage measurement https://doi.org/10.7795/550.20190509	DKD-L 02-2	
		Edition:	04/2014
		Revision:	0
		Page:	3 / 47

Suggestion for the quotation of the references:

*Guide DKD-L 02-02 Procedures for a traceable RF voltage measurement, Edition 04/2014, Revision 0, Physikalisch-Technische Bundesanstalt, Braunschweig and Berlin.
DOI: <http://dx.doi.org/10.7795/550.20190509>*

This document and all parts contained therein are protected by copyright and are subject to the Creative Commons user license CC by-nc-nd 3.0 (<http://creativecommons.org/licenses/by-nc-nd/3.0/de/>). In this context, “non-commercial” (NC) means that the work may not be disseminated or made publicly accessible for revenue-generating purposes. The commercial use of its contents in calibration laboratories is explicitly allowed.




Authors:

Members of the Technical Committee *High Frequency and Optics* of the DKD

Published by the Physikalisch-Technische Bundesanstalt (PTB) for the German Calibration Service (DKD) as result of the cooperation between PTB and the Technical Committee *High Frequency and Optics* of the DKD.

This document is a translation. The authoritative version is the original German Guide DKD-L 02-2 (edition 04/2014).

	<p>Procedures for a traceable RF voltage measurement</p> <p>https://doi.org/10.7795/550.20190509</p>	DKD-L 02-2	
		Edition:	04/2014
		Revision:	0
		Page:	4 / 47

Foreword

The DKD guides are recommendations on technical issues linked to the practical work of accredited calibration laboratories. The guides contain procedures which accredited calibration laboratories may use as a model for defining internal processes and regulations. DKD guides may become an essential component of the quality management manuals of calibration laboratories. By using these guides, the laboratories are enabled to put the respective state-of-the-art techniques into practice. This is intended to contribute to a harmonization of procedures as well as to improve the work efficiency in calibration laboratories.

The DKD guides should not impede the further development of calibration procedures and processes. Deviations from guides are allowed if there are technical reasons to support this action.

The present guide was prepared by the PTB Working Group *High-Frequency Measuring Techniques* at the request of the DKD Technical Committee *High Frequency and Optics*, and approved by the Board of the DKD.

The content of this document is largely based on records and internal worksheets of the PTB Working Group 2.22 *High-Frequency Measuring Techniques*, dealing on the subject of the measurand HF voltage. The aim is to provide a clear and comprehensive overview of the procedures for HF voltage measurement. While preparing this document, we tried to make sure that it can also be of use for persons who do not have extensive experience in metrology at higher frequencies. The document does not provide information on how to calculate the measurement uncertainty of the respective calibration procedures.



	Procedures for a traceable RF voltage measurement https://doi.org/10.7795/550.20190509	DKD-L 02-2	
		Edition:	04/2014
		Revision:	0
		Page:	5 / 47

Table of Contents

1. Introduction	6
2. Fundamentals of RF voltage measurement and calibration	7
2.1 Differences in contrast to the measurement of DC voltage and low frequency signals. 7	
2.2 Spatial dependence of RF voltage on waveguides	7
2.2.1 Reflection.....	7
2.2.2 Attenuation	9
2.3 Voltage transmission in voltage, current and impedance realization	9
2.4 Voltage transmission by means of a signal flow graph for the realization of power waves	11
2.5 Voltage changes along homogenous lines.....	13
2.5.1 Calculation.....	13
2.5.2 Approximation for short lines.....	15
2.5.3 Description by means of the reflection factor	17
3. Transfer and primary standards.....	18
3.1 Transfer standards for AC voltage calibration	18
3.2 RF voltage standard by traceability to RF power and RF impedance.....	20
3.3 Configuration of RF voltage standards.....	21
3.3.1 High-resistance thermal converters up to 100 MHz.....	22
3.3.2 Matched thermal converters.....	23
3.3.3 Thermal converters up to 1 GHz	24
3.3.4 Thermal converters for higher voltages	25
3.3.5 Thermal converters for current measurements.....	25
3.4 Modelling thermoelectric RF power sensors	27
3.4.1 Equivalent circuit of the sensor	28
4. Traceability of the measurand RF voltage	32
4.1 Traceability to the measurands reflection factor and calibration factor	33
4.2 Theoretical calculation of the input impedance of the NRS resistive sensor head.....	34
4.2.1 Power dependence of the absorption resistor	35
4.3 Determination of the effective efficiency of NRS sensor heads	35
5.1 Measurement by means of a T-junction	36
5.2 Measurement of the incident voltage by means of power splitters	37
5.3 RF voltage calibration of 50 Ω generators.....	38
5.4 Generation of low RF voltages.....	39
6. Calibration of thermal converters as RF voltage transfer standards.....	40
6.1 Measuring principle for DC substitution	40
6.2 Measuring principle for AC substitution.....	42
7. RF voltage calibration of oscilloscopes	45
8. Bibliography	46


	Procedures for a traceable RF voltage measurement https://doi.org/10.7795/550.20190509	DKD-L 02-2	
		Edition:	04/2014
		Revision:	0
		Page:	6 / 47

1. Introduction

Voltage, current and resistance are the basic measurands for precision measurements in the field of direct current and low frequency. At radio frequencies (RF), however, RF power and reflection are the most relevant, while voltage and current measurement only plays a secondary role. Accordingly, extensive literature can be found regarding the RF power and reflection measurement. Very little has been published about RF voltage measurement, which is equally the case for current measurement at higher frequencies. Voltage measurements from frequencies above approx. 1 MHz can be divided as follows:

Traditional measurement procedures prevail in the frequency range up to 100 MHz: the source voltage of low impedance sources is determined by high impedance voltage measurement. For frequencies above about 1 GHz, both voltmeters and sources are usually adapted to the characteristic impedance of the connecting lines, i.e. load and source impedance are identical (usually 50 Ω). Given the low source resistance, a voltage measurement without load proves difficult. As a matter of principle, procedures from both areas can be applied in the range between 100 MHz and 1 GHz. In the range above approx. 1 GHz, it is usually only the amplitude of the incident voltage wave which is measured. Taking into account the characteristic impedance of the incident power, it can be measured with high accuracy.

The present document describes the things to be considered in traceable RF voltage measurement in the frequency range above 1 MHz. In addition, there will be a brief discussion about RF current measurement.

	Procedures for a traceable RF voltage measurement https://doi.org/10.7795/550.20190509	DKD-L 02-2	
		Edition:	04/2014
		Revision:	0
		Page:	7 / 47

2. Fundamentals of RF voltage measurement and calibration

2.1 Differences in contrast to the measurement of DC voltage and low frequency signals

In the field of direct current and low frequency, electrical devices are usually optimized for the use in energy technology. The internal resistances R_i of the generators should be as small as possible, whereas by comparison the input resistances of the loads R_L are substantially higher, in order to reach values close to one for the energy efficiency during the energy transmission. Adequate high resistance voltmeters can be realized in this frequency range. Thus, the load on the source to be measured is negligibly small in these systems, and the open circuit voltage of the source can be measured with high precision. Moreover, the connecting cables between the point of measurement and the voltmeter are usually not affected (negligible voltage drop).

Devices and circuits for high frequency technology, however, are mainly used in telecommunications. They are specifically designed for this task, which is to provide a low-loss and distortion-free transmission of signals. For this purpose, the internal resistance of the generator, the input impedance of the receivers as well as the characteristic impedance of the connecting lines must have the same value (matched). With rising frequency, it becomes more and more difficult to realize high-impedance resistances (e.g. as input resistance of voltmeters), due to inevitable reactances. As a consequence, voltage measurement as potential difference – as is common in DC and low-frequency technology – causes difficulties in the high frequency range.

As nominal resistance, a value of 50Ω (partly 75Ω) for generator, load and line impedance is widely spread. This low working resistance in high-frequency technology makes voltage measurement in this frequency range difficult. Furthermore, the no longer sufficiently small propagation times at higher frequencies lead to periodic changes of the resulting voltage along the line. This already happens with only a small mismatch at the cable ends. In addition, the line attenuation, which increases according to the rising frequency, causes frequency-dependant voltage changes along the line and in the circuits. The lower the desired measurement uncertainty, the lower is the frequency limit above which these effects have to be taken into account.

2.2 Spatial dependence of RF voltage on waveguides

2.2.1 Reflection

The signal propagation on RF lines and in RF circuits can be described by means of voltage and current waves which are capable of propagating themselves in both directions along a line. The voltages and currents of these waves are linked to the characteristic impedance, for both the incident and the reflected wave [1]-[3]. By terminating a line with the impedance Z_L , which deviates from the line's characteristic impedance Z_0 , a reflected wave is caused which, by superposition with the incident wave, results in a standing wave field. As to the voltage, this leads to a periodic change along the line, with a periodicity corresponding to half the wavelength of the incident or the reflected wave. The complex amplitude (indicated by the underlined formula symbol) $\underline{U}_{\text{refl}}$ of the voltage wave, reflected by the mismatch at the cable ends, is calculated from the complex amplitude $\underline{U}_{\text{inc}}$ of the incident wave at the end of the line and the complex-valued reflection factor Γ :

$$\underline{U}_{\text{refl}} = \Gamma \cdot \underline{U}_{\text{inc}} \quad (2.1)$$

Where

$$\Gamma = \frac{Z_L - Z_0}{Z_L + Z_0} = |\Gamma| \cdot e^{j\phi_\Gamma} \quad (2.2)$$

For a small mismatch ($\Delta Z = Z_L - Z_0 \ll Z_0$) the approximation is

$$\Gamma \approx \frac{\Delta Z}{2Z_0} \quad (2.3)$$

Due to the different direction of movement with a continuously changing phase shift, the complex voltage amplitudes $\underline{U}_{\text{inc}}(x)$ and $\underline{U}_{\text{refl}}(x)$ superpose along the line, and thus form the resulting, spatially dependent voltage \underline{U}_x which varies periodically along the line, as is shown in figure 2.1.

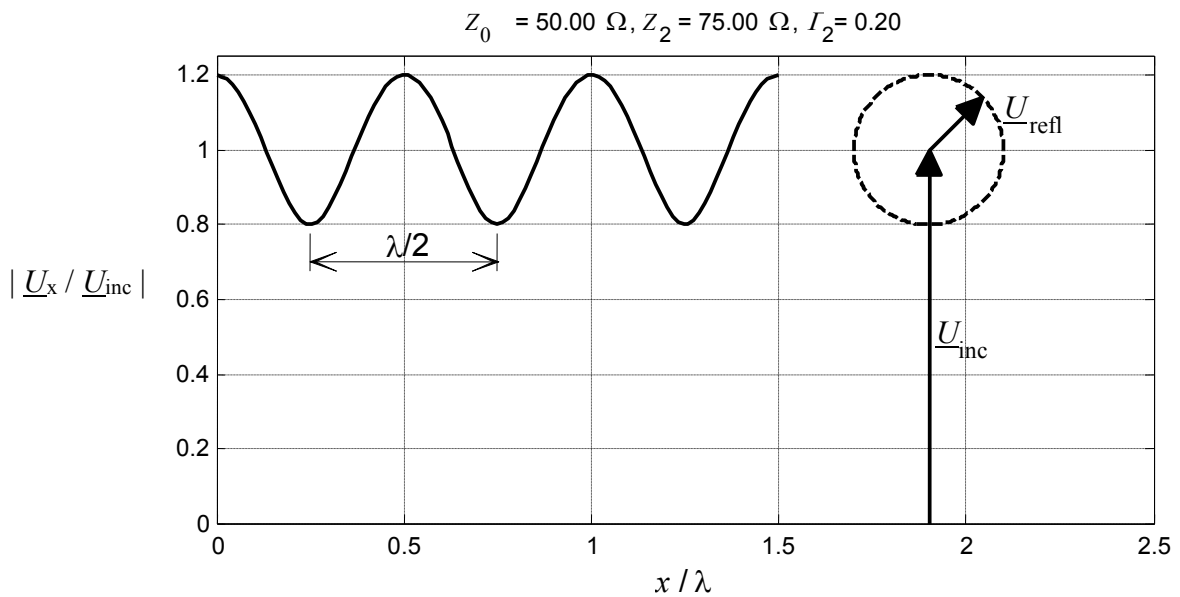



Figure 2.1: Periodic change of the normalized voltage amplitude \underline{U}_x along a line terminated by $Z_2 \neq Z_0$, due to the overlapping of the incident and the reflected wave.

The complex voltage amplitude \underline{U}_x at a point x on the line is the vectorial sum of the incident and the reflected voltage wave:

$$\underline{U}_x = \underline{U}_{\text{refl},x} + \underline{U}_{\text{inc},x} \quad (2.4)$$

By using the spatially dependent complex reflection factor Γ_x , you obtain

	Procedures for a traceable RF voltage measurement https://doi.org/10.7795/550.20190509	DKD-L 02-2	
		Edition:	04/2014
		Revision:	0
		Page:	9 / 47

$$\underline{U}_x = \underline{U}_{inc,x} (1 + \Gamma_x). \quad (2.5)$$

A deviation between the load impedance Z_L and the line resistance Z_0 leads to a spatially dependent variation between the maximum value U_{max} and the minimum value U_{min} . The ratio of U_{max} to U_{min} is called voltage standing wave ratio s (VSWR) and does not depend on the phase of the reflection factor Φ_Γ :

$$s = \frac{U_{max}}{U_{min}} = \frac{|\underline{U}_{inc}| + |\underline{U}_{refl}|}{|\underline{U}_{inc}| - |\underline{U}_{refl}|} = \frac{1 + |\Gamma|}{1 - |\Gamma|}. \quad (2.6)$$

Therefore, a specification of the voltage at higher frequencies (and thus shorter wavelengths) does only make sense when simultaneously defining a **reference plane**. At higher frequencies and according to the definition given above, even short line segments between components have to be considered as lines. For example, the ratio between the input voltage and the display of the voltmeter can change considerably by the insertion of an adapter.

2.2.2 Attenuation

Due to the finite conductivity and the dielectric losses, the attenuation of signals on coaxial lines increases with rising frequency. However, the influence on the voltage measurement is usually much lower than it would be in the case of a signal variation caused by mismatch. Even with a highly different conductivity, as is the case with brass (specific conductivity 15 MS/m) and silver (61 MS/m), the attenuation differences for the RF voltage up to 1 GHz only range from $2 - 4 \cdot 10^{-4}$, when using a 2 cm long adapter for PC 7 (typical length).

2.3 Voltage transmission in voltage, current and impedance realization

The low-ohmic resistance in high-frequency technology makes a precise voltage measurement at high frequencies more complex. This can be illustrated by way of an example: a generator G with an open circuit voltage \underline{U}_S and an internal resistance Z_L is connected to a load resistor (input resistance of a device) (Fig. 2.2). It is assumed that: $Z_G = Z_0$ and $Z_L = Z_0 + \Delta Z_L$ with $\Delta Z_L \ll Z_0$, which means that the load is slightly mismatched.

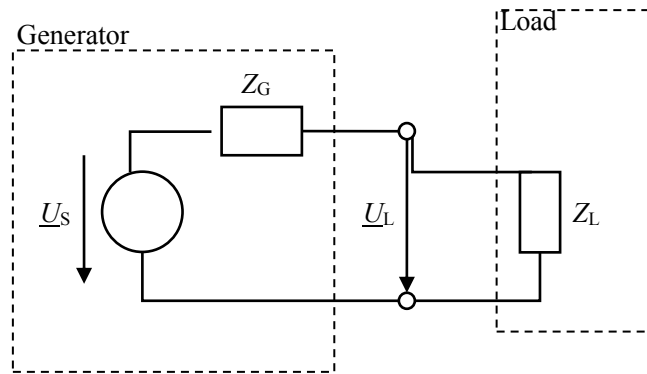


Figure 2.2: Equivalent circuit diagram of the interconnection of a generator (open circuit voltage U_s and internal resistance Z_G) with a load impedance Z_L .

The voltage U_L across Z_L can be calculated from the relation

$$\frac{U_s}{U_L} = \frac{Z_G + Z_L}{Z_L} \quad (2.7)$$

by the voltage division at impedances. If $Z_L = Z_G = Z_0$, then it results that $U_L = U_s/2$. Introducing the voltage U_{Z_0} , it is the voltage if $Z_L = Z_0$, then the voltage across Z_L is for $Z_G = Z_0$ is $U_{Z_0} = U_s/2$.

Assuming the general case of a small mismatch, the result of an approximate calculation is:

$$U_L \approx U_{Z_0} \left(1 + \frac{\Delta Z_L}{2Z_0} \right) \quad (2.8)$$

with

$$\Delta Z_L = Z_L - Z_0. \quad (2.9)$$

Setting up the equation

$$U_L = U_{Z_0} + \Delta U_L, \quad (2.10)$$

it follows that:

$$\frac{\Delta U_L}{U_{Z_0}} \approx \frac{1}{2} \frac{\Delta Z_L}{Z_0}. \quad (2.11)$$

In case of a small mismatch, the relative deviation of the voltage value U_L from the value in the case of match U_{Z_0} equals half the relative deviation of the value of the load impedance from the nominal value Z_0 . A corresponding approximate calculation shows that the relative change of the active power P_L at Z_L is small when there is a small mismatch of the load impedance of a higher order. With

$$P_{Z_0} = \frac{U_{Z_0}^2}{2Z_0} \quad (2.12)$$

it follows that:

$$P_L \approx P_{Z_0} \left| 1 - \left(\frac{\Delta Z}{2Z_0} \right)^2 \right|. \quad (2.13)$$

Neglecting a small mismatch thus leads to substantially greater measurement errors for the voltage than it does for the real power.

An exact broadband adjustment of both the generator and the load impedance to Z_0 is difficult to realize. Therefore, the output voltage of generators is always slightly different. When measuring the output voltage of a generator, it is therefore common practice to indicate the voltage \underline{U}_{Z_0} which the generator delivers at the nominal impedance $Z_0 = 50 \Omega$ (see section 7.1). This is, for example, a common process for function generators and oscilloscope calibrators.

2.4 Voltage transmission by means of a signal flow graph for the realization of power waves

The calculation of the voltage transmission between a generator and a load (as described in the example in section 2.3) can be carried out at high frequencies with the help of a signal flow graph and power waves. Even in case of a mismatched generator, it facilitates a clear description of the procedures. Here, the connection between the generator and the load is modelled by a lossless line (ideal transmission factor 1). The propagation processes on this line are described by the superposition of an incident and a reflected power wave [1]. The circuit for calculating the voltage transmission of the example in section 2.3 – here by means of a signal flow graph with power waves – is shown in figure 2.3, without a HF line.

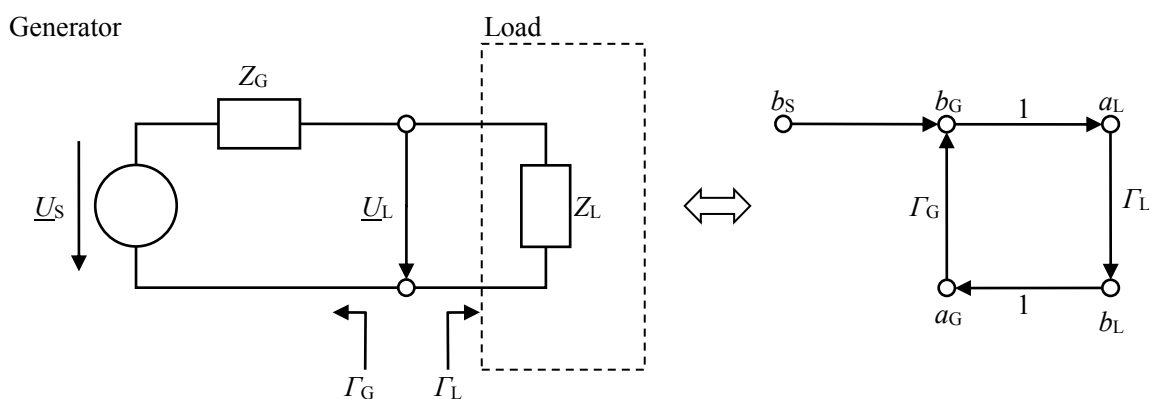


Figure 2.3: Equivalent circuit diagram of the interconnection of a generator with a load and corresponding signal flow graph.

The incident and reflected waves between generator and load are described by the power waves a and b , with a being a wave directed towards the load and b a wave returning from the load. Accordingly, the waves have been assigned reversed designations in relation to the generator G and the load L . For the present case, that is to say the direct connection between generator and load, this means: $a_L = b_G$ und $a_G = b_L$. Γ_G is the reflection factor at the output port of the generator (when looking into the generator), Γ_L the one at the input port of the load. The generator is thus characterized by its reflection factor Γ_G and the incident power wave b_S , directed at an ideal impedance (Z_0). The relationship between the complex amplitudes of the incident wave $\underline{U}_{\text{inc}}$ and the reflected power wave $\underline{U}_{\text{refl}}$, for example at the port of the load, and the corresponding power waves a_L and b_L is defined as:

$$a_L = \frac{\underline{U}_{\text{inc}}}{\sqrt{Z_0}} \quad \text{and} \quad b_L = \frac{\underline{U}_{\text{refl}}}{\sqrt{Z_0}}. \quad (2.14)$$

The power waves are the voltages that are standardized to the root of the real nominal characteristic impedance Z_0 of the line system. Thus, the square values of the power waves a and b yield the incident power P_{inc} and the reflected power P_{refl} :

$$P_{\text{inc}} = \frac{1}{2}|a|^2 \quad \text{and} \quad P_{\text{refl}} = \frac{1}{2}|b|^2. \quad (2.15)$$

The following applies for the incident power wave b_S (also called primary wave) of an ideal generator ($Z_G = Z_0$) connected to an ideal load ($Z_L = Z_0$, i. e. $\Gamma_L = 0$):

$$b_S = \frac{\underline{U}_{Z_0}}{\sqrt{Z_0}}. \quad (2.16)$$

Under not ideal conditions ($Z_G \neq Z_0$) the relation is [1]:

$$b_S = \frac{\underline{U}_S \sqrt{Z_0}}{Z_0 + Z_G}. \quad (2.17)$$

As described in section 2.2, the voltage amplitude at a line termination is determined as a superposition of the two complex amplitudes of the incident and the reflected wave. The voltage at the input port of the load L is therefore calculated according to Figure 2.3

$$\underline{U}_L = \underline{U}_{\text{inc}} + \underline{U}_{\text{refl}} = (a_L + b_L)\sqrt{Z_0}. \quad (2.18)$$

If $b_L = a_L \Gamma_L$ then


$$\underline{U}_L = a_L(1 + \Gamma_L)\sqrt{Z_0}, \quad (2.19)$$

and with equation (2.14):

$$\underline{U}_L = \underline{U}_{\text{inc}}(1 + \Gamma_L). \quad (2.20)$$

When adjusting ($\Gamma_L = 0$) then $a_L = b_S$, from which follows that:

$$|\underline{U}_{L,Z_0}| = |b_S|\sqrt{Z_0} = \underline{U}_{Z_0}. \quad (2.21)$$

	Procedures for a traceable RF voltage measurement https://doi.org/10.7795/550.20190509	DKD-L 02-2	
		Edition:	04/2014
		Revision:	0
		Page:	13 / 47

In comparison to section 2.3, the voltage $\underline{U}_{\text{inc}}$ reappears when using the signal flow graph for calculation. This voltage amplitude $\underline{U}_{\text{inc}}$ of the incident wave on the gate is linked in a simple way to the incident power P_{inc} on the load:

$$\underline{U}_{\text{inc}} = \sqrt{2P_{\text{inc}}Z_0} \quad (2.22)$$

The relation between the wave quantity a_L and the generator wave b_S can be calculated from the power wave graph

$$a_L = \frac{b_S}{|1 - \Gamma_G \Gamma_L|} \quad (2.23)$$

Thus, the relation between the reference power P_{Z_0} of the generator and the incident power P_{inc} is given:

$$P_{\text{inc}} = \frac{P_{Z_0}}{|1 - \Gamma_G \Gamma_L|^2} \quad (2.24)$$

The value of the incident power P_{inc} therefore depends on the reflection factor of the generator and the reflection factor of the load. Since

$$\underline{U}_{Z_0} = \sqrt{2P_{Z_0}Z_0} \quad (2.25)$$

the simple relation between the three voltages at the input port of the load can be specified:

$$\underline{U}_{\text{inc}} = \frac{\underline{U}_{Z_0}}{|1 - \Gamma_G \Gamma_L|} \quad (2.26)$$

$$\underline{U}_L = \frac{\underline{U}_{Z_0}(1 + \Gamma_L)}{|1 - \Gamma_G \Gamma_L|} \quad (2.27)$$

The equations (2.25), (2.26) and (2.27) together with equation (2.22) are essential for the precise analysis of the calibrations with RF voltages. **RF power meters are always calibrated with reference to the incident power P_{inc} .** After a conversion based on Z_0 , according to equation (2.22), the voltage displayed therefore always corresponds to the **incident voltage $\underline{U}_{\text{inc}}$.**

2.5 Voltage changes along homogenous lines

If a line is not terminated with its characteristic impedance, the incident and the reflected wave on the line superpose each other and, as a consequence, the resulting voltage along this line will change.

2.5.1 Calculation

Let us assume that a short line (length l) is terminated on its output side (port 2) with a voltmeter having the input impedance Z_2 . The input voltage U_2 is displayed on the voltmeter's main-frame. The subsequently derived formula can be used to determine the voltage difference between port 1 and port 2, when moving the reference plane of the voltage measurement from point 1 to point 2 (e.g. upon removal of an inserted adapter). The aim of the calculation is to establish a relationship between the voltage U_2 at the end of the line and the voltage U_x at point x on the line.

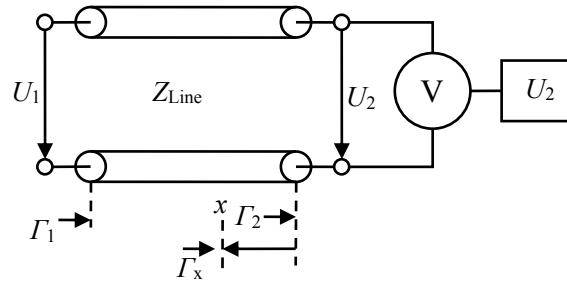


Figure 2.4: Equivalent circuit diagram of a line with connected voltmeter.

By using the reflection factor

$$\Gamma_2 = |\Gamma_2| e^{j\phi_2} = \frac{U_{2,\text{refl}}}{U_{2,\text{inc}}} = \frac{Z_2 - Z_{\text{Line}}}{Z_2 + Z_{\text{Line}}} \quad (2.28)$$

at the end of the line (port 2), voltage \underline{U}_2 is obtained at port 2 from the vectorial sum of the incident and reflected amplitude:

$$|\underline{U}_2| = |\underline{U}_{\text{refl},2} + \underline{U}_{\text{inc},2}| = |\underline{U}_{\text{inc},2}| \cdot |1 + \Gamma_2| \quad (2.29)$$

Going back on the line by a length x towards the generator, the phase Φ of the reflection factor changes. The line attenuation is being neglected. At a distance x from port 2, the following equation applies for the reflection factor:

$$\Gamma_X = \Gamma_2 \cdot e^{-2j\beta x} = |\Gamma_2| \cdot e^{j(\Phi_2 - 2\beta x)}, \quad (2.30)$$

with the propagation constant $\beta = 2\pi / \lambda$. In a coaxial line, the electrical length x results from the mechanical length x_{mech} according to $x = x_{\text{mech}} \sqrt{\epsilon_r}$, with ϵ_r being the relative dielectric constant of the power dielectric (e.g.: $\epsilon_r = 1,000649$ for air). For the voltage \underline{U}_x at a distance x from the port 2, the following applies:

$$|\underline{U}_x| = |\underline{U}_{\text{inc},x}| \cdot |1 + \Gamma_x|. \quad (2.31)$$

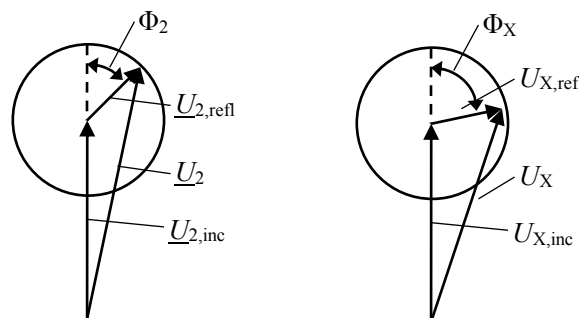


Figure 2.5: Vector representation of the voltages on the line from Figure 2.4

Using the law of cosine, the results from Figure 2.5 are:

$$|U_2| = |U_{inc,2}| \cdot \sqrt{1 + |\Gamma_2|^2 + 2|\Gamma_2| \cos \Phi_2} \quad (2.32)$$

$$|U_x| = |U_{inc,x}| \cdot \sqrt{1 + |\Gamma_2|^2 + 2|\Gamma_2| \cos(\Phi_2 - 2\beta x)} \quad (2.33)$$

and the result for the ratio of the voltages is:

$$\frac{|U_x|}{|U_2|} = \frac{|U_{inc,x}|}{|U_{inc,2}|} \cdot \frac{\sqrt{1 + |\Gamma_2|^2 + 2|\Gamma_2| \cos(\Phi_2 - 2\beta x)}}{\sqrt{1 + |\Gamma_2|^2 + 2|\Gamma_2| \cos \Phi_2}} \quad (2.34)$$

With $|\Gamma| \ll 1$ and at a low attenuation, i.e. $|U_{inc,x}| \approx |U_{inc,2}|$, we obtain the approximation

$$\frac{|U_x|}{|U_2|} \approx \sqrt{1 + 2|\Gamma_2| \cos(\Phi_2 - 2\beta x) - \cos \Phi_2} \approx 1 + |\Gamma_2| \cos(\Phi_2 - 2\beta x) - \cos \Phi_2 \quad (2.35)$$

Often, only the relative deviation $|\Delta U_{2-x}|$ between the two voltages $|U_x|$ and $|U_2|$ is of interest. The result of $|U_x| = |U_2| + |\Delta U_{2-x}|$ is:

$$\begin{aligned} \frac{|\Delta U_{2-x}|}{|U_2|} &\approx |\Gamma_2| |\cos(\Phi_2 - 2\beta x) - \cos(\Phi_2)| \\ &\approx |\Gamma_2| |\cos(\Phi_2) \cdot [\cos(2\beta x) - 1] + \sin(\Phi_2) \cdot \sin(2\beta x)|. \end{aligned} \quad (2.36)$$

2.5.2 Approximation for short lines

Based on the transmission theory, the following input impedance for a line of a length l , with the terminating impedance Z_2 , the characteristic impedance Z_{Line} and the propagation constant γ can be deduced

$$Z_1 = Z_{Line} \frac{\frac{Z_2}{Z_{Line}} + \tanh(\gamma l)}{1 + \frac{Z_2}{Z_{Line}} \tanh(\gamma l)} \quad (2.37)$$

For lines with low losses ($\alpha \ll \beta$, $\tanh \gamma l \approx \tanh \beta l \approx j \tan \beta l$) we obtain the approximation:

$$Z_1 \approx Z_{Ltg} \frac{\frac{Z_2}{Z_{Line}} + j \tan \beta l}{1 + j \frac{Z_2}{Z_{Line}} \tanh \beta l} \quad (2.38)$$

For electrically short lines with $\beta l \ll 1$ we obtain:

$$Z_1 \approx Z_{\text{Line}} \frac{\frac{Z_2}{Z_{\text{Line}}} + j\beta l}{1 + j \frac{Z_2}{Z_{\text{Line}}} \beta l}. \quad (2.39)$$

For the voltage \underline{U}_1 at the input of a line the following applies:

$$\underline{U}_1 = \underline{U}_2 \left(\cosh \gamma l + \frac{Z_{\text{Line}}}{Z_2} \sinh \gamma l \right). \quad (2.40)$$

For low-loss lines ($\alpha \ll \beta$, $\cosh \gamma l \approx \cos \beta l$ und $\sinh \gamma l \approx j \sin \beta l$) the following approximation is made:

$$\underline{U}_1 \approx \underline{U}_2 \left(\cos \beta l + j \frac{Z_{\text{Line}}}{Z_2} \sin \beta l \right), \quad (2.41)$$

And at low frequencies, due to $\beta l \ll 1$, we obtain:

$$\underline{U}_1 \approx \underline{U}_2 \left(1 - \frac{(\beta l)^2}{2} + j \frac{Z_{\text{Line}}}{Z_2} \beta l \right). \quad (2.42)$$

With $Y_{\text{Line}} = \frac{1}{Z_{\text{Line}}}$ and $Y_2 = \frac{1}{Z_2} = G_2 + jB_2$, equation (2.42) can also be circumscribed:

$$\underline{U}_1 \approx \underline{U}_2 \left(1 - \frac{B_2}{Y_{\text{Line}}} \beta l - \frac{(\beta l)^2}{2} + j \frac{G_2}{Y_{\text{Line}}} \beta l \right). \quad (2.43)$$

Equation (2.36) can also be simplified for short lines. When $x < 0,05\lambda$ (e.g. $x < 15$ mm at 1 GHz) it follows that:

$$\frac{|\Delta U_{2-L}|}{|U_2|} \approx |\Gamma_2| \cdot 4\pi \frac{l}{\lambda} \left[\sin(\Phi_L) - 2\pi \frac{l}{\lambda} \cos(\Phi_L) \right]. \quad (2.44)$$

At 1 GHz, the deviation derived by the approximations is less than 10 %.

For example, Figure 2.6 shows the relative voltage change when shifting the reference plane by 10 mm (e.g. adapter). The parallel connection of a resistance ($R = 51 \Omega$) and a capacitance $C = 0,05$ pF is assumed as input impedance of the voltmeter. The following figure shows a good agreement when using the equations (2.36) and (2.44).

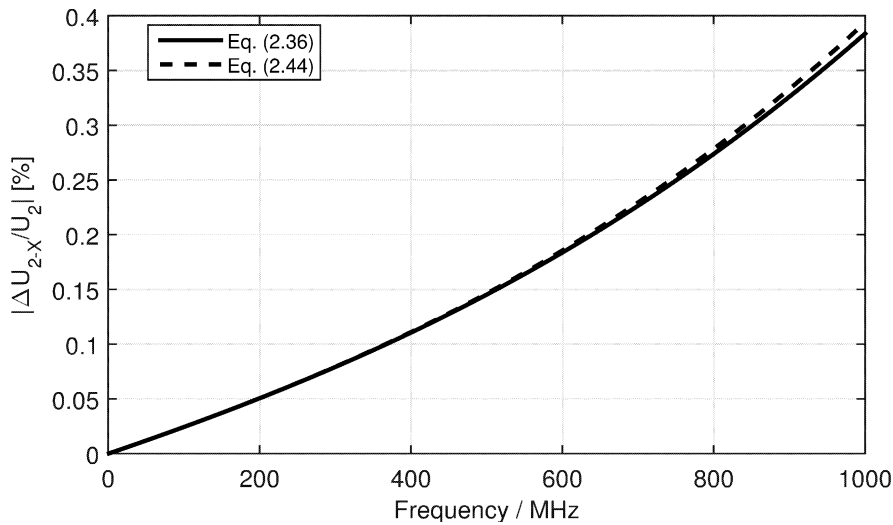


Figure 2.6: Relative voltage change when shifting the reference plane of a mismatched sensor head (51 Ω parallel to 50 fF) by 10 mm.

2.5.3 Description by means of the reflection factor

The equation

$$\Gamma_1 = \Gamma_2 \cdot e^{-2\gamma l} \quad (2.45)$$

describes the transformation of the reflection factor along the line, and indicates the relation between the reflection factor Γ_1 at the beginning and Γ_2 at the end of the line. The reflection factor Γ_2 at the end of the line is calculated from the characteristic line impedance Z_{Line} and the terminating impedance Z_2 according:

$$\Gamma_2 = \frac{\underline{U}_{\text{refl},2}}{\underline{U}_{\text{inc},2}} = \frac{Z_2 - Z_{\text{Line}}}{Z_2 + Z_{\text{Line}}} \quad (2.46)$$


It follows from equation (2.45) that:

$$\begin{aligned} \underline{U}_1 &= \underline{U}_{\text{inc},1}(1 + \Gamma_1) \\ \underline{U}_2 &= \underline{U}_{\text{inc},2}(1 + \Gamma_2) \end{aligned} \quad (2.47)$$

For the ratio $\underline{U}_1 / \underline{U}_2$ this means

$$\frac{\underline{U}_1}{\underline{U}_2} = \frac{\underline{U}_{\text{inc},1}}{\underline{U}_{\text{inc},2}} \frac{(1 + \Gamma_1)}{(1 + \Gamma_2)}, \quad (2.48)$$

and according to the transmission theory, it is valid that

	Procedures for a traceable RF voltage measurement https://doi.org/10.7795/550.20190509		DKD-L 02-2	
			Edition:	04/2014
			Revision:	0
			Page:	18 / 47

$$\underline{U}_{\text{inc},2} = \underline{U}_{\text{inc},1} e^{-\gamma l}, \quad (2.49)$$

which means that:

$$\frac{\underline{U}_1}{\underline{U}_2} = e^{\gamma l} \frac{(1 + \Gamma_1)}{(1 + \Gamma_2)}. \quad (2.50)$$

With equation (2.45), we obtain:

$$\frac{\underline{U}_1}{\underline{U}_2} = e^{\gamma l} \frac{(1 + \Gamma_2 e^{-2\gamma l})}{(1 + \Gamma_2)}. \quad (2.51)$$

This formula is useful when the final complex reflection coefficient can be accurately measured and the data of the line (or the adapter) are known or can be estimated.

3. Transfer and primary standards

3.1 Transfer standards for AC voltage calibration

The quantity of DC voltage in the range between 1 V and 10 V can be realized with a very low relative measurement uncertainty of about 10^{-8} (coverage factor $k = 2$). This is possible due to the fact that it can be traced back to fundamental constants and the quantity of frequency by means of a quantum primary standard based on the Josephson effect. The realization of AC voltages with a similarly low measurement uncertainty in the lower kHz range is also possible. This is done by synthesizing sinusoidal alternating voltages from exact fast switching DC voltage impulses. This method, however, is not yet applicable for alternating voltages of higher frequencies, since very high switching speeds are required. Here, precise AC voltage measurements have to be traced back to known DC voltages by means of transfer standards. In these transfer standards, the real power, which is caused by the AC voltage in a frequency-independent resistance, is compared to an equivalent DC power. A temperature sensor at the resistor detects the generated heating, which is displayed on a measuring instrument. As shown in Figure 3.1, a so-called thermal converter is used for this purpose. After amplification, its thermal voltage U_{th} is displayed on a digital voltmeter. Since the thermal effect is used only for comparison, an absolute calibration of the temperature measurement is not necessary. Due to the comparison of the real power, it is always the **effective value** of the alternating voltage that is measured.

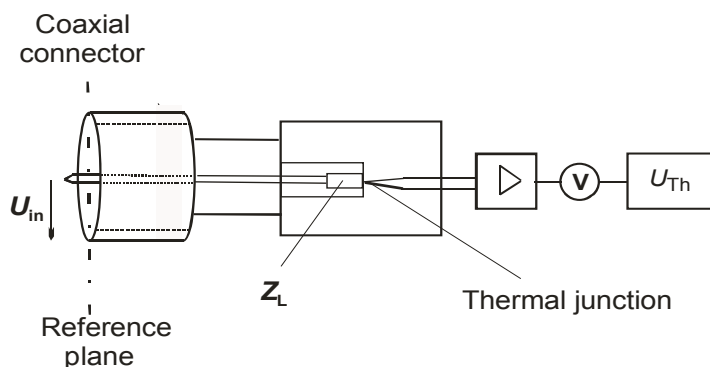


Figure 3.1: Schematic diagram of a transfer standard for the traceability of an AC voltage to a DC voltage

Up to approx. 1 MHz, it is possible to realize transfer standards with a planar resistance (some 100 Ω) and integrated thermal elements (also called thermopile when connected in series) for highly accurate temperature detection [4]. Up to approx. 1 MHz, the relative deviation between the AC and DC resistance ranges from $1 \cdot 10^{-6}$ to $1 \cdot 10^{-5}$. Thus, AC voltage measurements – which are traceable to a precisely known DC voltage – are possible with these relative measurement uncertainties, and without exact knowledge of the resistance values.

The AC-DC voltage transfer difference δ_{DC} is defined as the characteristic quantity of the AC voltage transfer standards. It is a measure for the difference between the AC voltage and the equivalent DC voltage, which both produce the **same output display** (e.g. thermal voltage U_{Th}).

The transfer difference δ_{DC} is calculated from AC and DC voltage:

$$\delta_{DC} = \frac{U_{AC} - U_{DC}}{U_{DC}} = \frac{U_{AC}}{U_{DC}} - 1. \quad (3.1)$$

The same transfer quantity is also used for RF voltage measurements. However, instead of a DC voltage, a low-frequency AC voltage (100 kHz to 1 MHz) is often chosen as reference frequency. At a reference frequency of 100 kHz, for example, the high-frequency AC transfer difference δ_{AC} is marked by the symbol δ_{100kHz} . This reference frequency is justified by fact that the lower cut-off frequencies of RF generators are usually in the upper kHz frequency range, and thus, only one generator is required for the measurement.

The relation between the DC and AC transfer difference for RF voltages is as follows:

$$\begin{aligned} \delta_{DC}(f) &= \frac{U_{HF}(f)}{U_{DC}} - 1 \\ &= \frac{U_{HF}(f)}{U_{AC}(100kHz)} \cdot \frac{U_{AC}(100kHz)}{U_{DC}} - 1 \\ &= (\delta_{100kHz}(f) + 1) \cdot (\delta_{DC}(100kHz) + 1) - 1 \\ &= \delta_{100kHz}(f) \cdot \delta_{DC}(100kHz) + \delta_{DC}(100kHz) + \delta_{100kHz}(f). \end{aligned} \quad (3.2)$$

For $\delta_{100kHz}(f) \ll 1$ and $\delta_{DC}(100kHz) \ll 1$ the following approximation applies:

$$\delta_{DC}(f) \approx \delta_{DC}(100kHz) + \delta_{100kHz}(f). \quad (3.3)$$

If thermal converters for higher frequencies show very small values for $\delta_{DC}(100kHz)$, then a further approximation can be introduced for $f \gg 100kHz$:

$$\delta_{DC}(f) \approx \delta_{100kHz}(f). \quad (3.4)$$

With the above-mentioned definitions, all DC and AC coupled thermal **power sensors** can be used as RF voltage transfer standards in the RF range. The power indication of the power measuring device can be used as output display, and, in the case of RF resistance sensor heads with bridge circuit, the bridge detuning can be used for temperature measurement.

3.2 RF voltage standard by traceability to RF power and RF impedance

For frequencies above approx. 1 MHz, the difference between the DC and RF value of the terminating resistance Z_L rises significantly. Besides, with a rising frequency, frequency-dependent losses in the supply line between the input port and the comparator resistance Z_L become apparent. In order to allow the use of transfer standards at frequencies above 1 MHz, the line losses and the RF resistance have to be measured frequency-dependently, and must then be used for correction. In the RF range, traceable resistance measurements can only be realized for 50 Ω or 75 Ω systems. The same is valid for RF power meters (traceable to microcalorimeters) in this range. Therefore, only transfer standards showing this kind of input resistances can serve as traceable primary standards for RF voltage. After careful measurement and correction of the reading, they can be used as primary standards for RF voltage at frequencies between 1 MHz and approx. 1 GHz.

For traceable calibration of RF power sensors in microcalorimeters, the effective efficiency η_{eff} is determined as the characteristic value. This characteristic value is the ratio of the absorbed RF power at the input port $P_{\text{RF,abs}}$ to the equivalent DC power P_{DC} or a low-frequency AC reference power P_{AC} , which causes identical heating at the RF-absorbing element.

$$\eta_{\text{eff}} = \frac{P_{\text{DC}}}{P_{\text{RF,abs}}} \Bigg|_{\text{constant indication}} \quad (3.5)$$

The input impedance Z_{in} of the sensor can be regarded as the series circuit of an active resistance R_{in} and a reactance X_{in} . The realization as input admittance Y_{in} is also common, a parallel circuit of conductance G_{in} and susceptance B_{in} :

$$Z_{\text{in}} = R_{\text{in}} + jX_{\text{in}} \quad (3.6)$$

$$Y_{\text{in}} = \frac{1}{Z_{\text{in}}} = G_{\text{in}} + jB_{\text{in}} \quad (3.7)$$

With the presentation by a conductance, the following simple relations are given for the RF power absorbed in the sensor $P_{\text{RF,abs}}$ and the equivalent DC power P_{DC}

$$P_{\text{DC}} = U_{\text{DC}}^2 \cdot G_{\text{DC}} \quad (3.8)$$

$$P_{\text{RF,abs}}(f) = U_{\text{RF,in}}^2(f) \cdot G_{\text{RF,in}}(f) \quad (3.9)$$

For the effective value of the RF input voltage this implies:

$$U_{\text{RF,in}}(f) = U_{\text{DC}} \cdot \sqrt{\frac{G_{\text{DC}}}{G_{\text{RF,in}}(f)}} \cdot \sqrt{\frac{1}{\eta_{\text{eff}}(f)}} \quad (3.10)$$

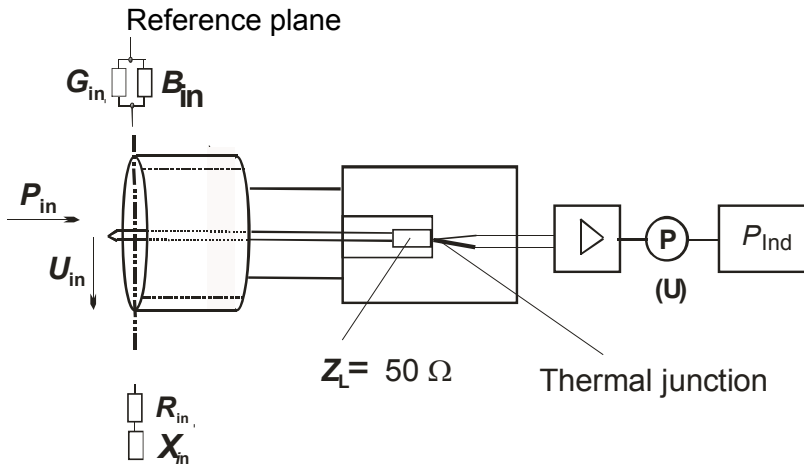


Figure 3.2: Transfer standard for RF voltage with a 50 Ω input resistance.

The effective value of the RF voltage $U_{RF,in}$ at the input port of the power sensor is calculated from the equivalent DC voltage, after correction of the frequency-dependent input conductance with relation to the DC voltage conductance. The frequency-dependent losses η_{eff} in the sensor head also have to be considered. For power sensors, whose frequency range does not extend down to DC, the HF power can be substituted by a low-frequency alternating power. The DC values will then be replaced by the AC values in the corresponding equations.

Equivalently, a power sensor head can also be used as a traceable RF current standard. When using the description of the real part of the input impedance by the resistance $R_{RF,in}$, the following applies for the effective value of the RF input current $I_{RF,in}$:

$$I_{RF,in}(f) = I_{DC} \cdot \sqrt{\frac{R_{DC}}{R_{RF,in}(f)}} \cdot \sqrt{\frac{1}{\eta_{eff}(f)}} \quad (3.11)$$

The effective value of the RF current, which flows into the input port of the power sensor, is calculated from the equivalent DC input current, after having corrected the frequency-dependent input resistance and the frequency-dependent losses η_{eff} in the sensor head.

After determination of the input impedance and the effective efficiency, a long-term stable RF power meter can be used as primary RF voltage or RF current standard. The reference plane is equal to the reference plane of the impedance measurement. If the measurands RF power (effective efficiency) and RF impedance have been traced back to primary standards, then a primary RF voltage or standard RF current can be realized. (See chapter 3.4).

3.3 Configuration of RF voltage standards

In the frequency range up to 1 GHz, thermal converters are used as transfer standards for RF voltage as well as for RF current. As opposed to diode voltmeters [5], thermal converters are characterized by their DC coupling, small transfer differences at low frequencies and their often monotonous frequency-response curves up to high frequencies. The latter facilitates the good interpolation of measuring values. Due to their configuration, they are durable and often used as reference standards in calibration laboratories. Compared to diode voltmeters, however, their dynamic range is very limited ($U_{max}/U_{min} \approx 2,5$). There are thermal converters with a matched input impedance of 50 Ω or 75 Ω , but often also much higher, as is customary with transfer standards in low frequency technology.

3.3.1 High-resistance thermal converters up to 100 MHz

As shown in Figure 3.3, a typical thermal converter up to 100 MHz consists of a range resistor R_{ran} and a series-connected thermocouple (TC), installed in a coaxial enclosure.

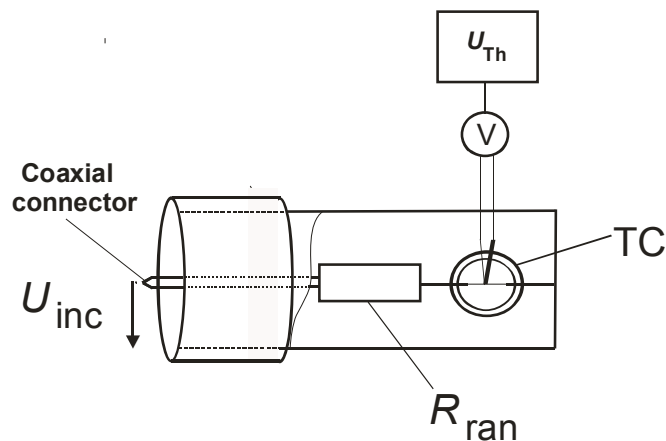


Figure 3.3: Principle of a thermal converter with a high-resistance input impedance for frequencies up to 100 MHz.

Thermal couples for RF applications are generally composed of a thin heating filament with an approximate diameter of $10\ \mu\text{m}$ and a resistance of approximately $100\ \Omega$. The nominal current lies in the range of $5\ \text{mA}$. The heating filament is fused inside a glass enclosure, together with an isolated thermocouple. A range resistor, which is set in front of the converter, limits the current for the different voltage measurement ranges, so that the value of $5\ \text{mA}$ will not be exceeded. Thus, the ratio between input resistance and nominal voltage is approx. $200\ \Omega/\text{V}$. Thermal converters up to 100 MHz for nominal voltages between $0,5\ \text{V}$ und $100\ \text{V}$ are commercially available. In the past, the more sexless type GR-874 played a dominant role as coaxial input connector, whereas today there is a clear preference for N connectors. We must always be aware that it is only in the lower dynamic range that the initial thermal voltage is exactly proportional to the power. This proportionality factor drops below 1 when approaching the nominal voltage. However, this deviation does not influence measurements of transfer differences carried out according to the definition set up for output responses.

High-resistance thermal converters cause a strong mismatch in $50\ \Omega$ systems. This, in turn, leads to a ripple of the voltage along the line which increases with rising frequency. Therefore, compliance with the voltage reference level is highly essential for accurate measurements.

3.3.2 Matched thermal converters

In matched thermal converters, a parallel resistance R_{par} (or a matching network) in front of the range resistor R_{ran} provides an input impedance of $Z_{\text{in}} \approx 50 \Omega$ (see Figure 3.4). However, the heating of the resistors limits the nominal values of these converters to $U_{\text{Nom}} \approx 3 \text{ V}$.

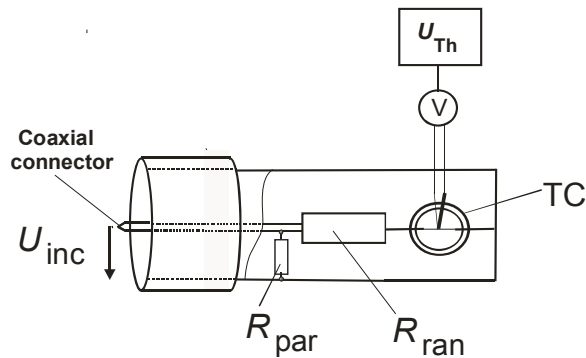


Figure 3.4: Matched thermal converter.

Matched converters are used, for example, in voltage calibrations of generators which operate on 50Ω loads.

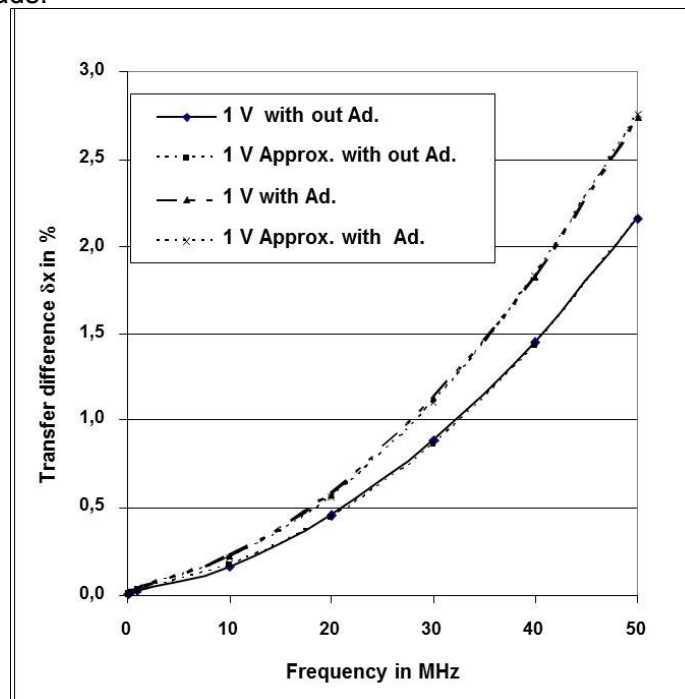


Figure 3.5: Measured transfer difference δ_x of a matched converter for 1 V with BNC connector, without and with adapter (25 mm) and approximations.

Figure 3.5 shows the measured transfer difference of a 50Ω converter with BNC connector, without and with an adapter (approx. 25 mm in length) in front. In addition, the measured values are approximated by an equation of the form $\delta_x(f) = k_1\sqrt{f} + k_2f^2$. The term $k_1\sqrt{f}$

takes into account the losses which are based on the skin effect, while $k_2 f^2$ takes into account the unavoidable reactances [6]. It can be seen that in both cases a very good approximation of the measured values is possible. Often, this approximation also applies for high-resistance converters. It turns out that the skin effect can be neglected for converters with input resistances above 500 Ω . These approximations are only possible for converters whose frequency response is not matched with additional components.

The distance between the curves, with and without adapter, indicates how the transfer difference is changed by the adapter. It rises with increasing frequencies and reaches approx. 2.5 % at 50 MHz. Therefore, precise measurements require a strict adherence to the reference plane. This is also the case for adapted converters.

3.3.3 Thermal converters up to 1 GHz

As is the case in the low frequency range, thermal converters in the RF range are calibrated by parallel connection with a reference standard, using a coaxial T-junction (see section 6.1). There are special high-resistance converters with an integrated T-junction facilitating the use of thermal converters up to 1 GHz as long-term stable reference standards. Due to different lengths of the T-junction's side arms, voltage changes will be avoided thereby. This implies that the converter has previously been calibrated against a voltage standard N. This converter, in combination with a RF generator, represents a RF voltage source with known values related to its reference plane (see Figure 3.6).

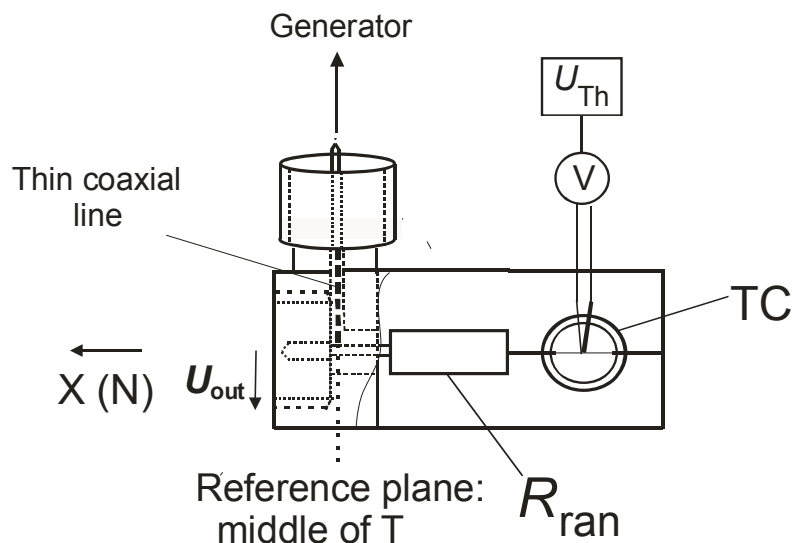



Figure 3.6: Thermal converter for frequencies up to 1 GHz, with integrated T-junction.

A 1 GHz converter also facilitates the calibration of thermal converters with relation to the reference plane in the centre of a commercial T-junction. For this purpose, a short piece of N-line is put at the output of the converter. With regard to its electrical length, the N-line corresponds exactly to the side arm of a commercial T-junction.

Up to approx. 100 MHz, 1 GHz converters show a frequency dependence in the transfer difference which we already know from the converters in chapter 3.3.2. In the range above 100 MHz, there can also be a decreasing frequency response. The relative transfer difference may be up to 20 %. The typical nominal voltages are 1 V, 2,5 V and 7 V [7].

	Procedures for a traceable RF voltage measurement https://doi.org/10.7795/550.20190509	DKD-L 02-2	
		Edition:	04/2014
		Revision:	0
		Page:	25 / 47

3.3.4 Thermal converters for higher voltages

In RF technology, the advantage of high-impedance converters is that, at higher voltages, they only require a lower power. In a 50 Ω system, a measuring device would consume approx. 200 W at 100 V. But in the case of a thermal converter with a measured current of 5 mA, it would be only 0.5 W.

As already mentioned in section 3.3.1, measuring ranges above 0.5 V for voltage converters are realized by putting series resistors in front of the thermocouple. For frequencies up to 100 MHz, the usual equipment consists of converters up to 100 V. The two lower voltage ranges (0.5 V and 1 V) are calibrated with low power, using a RF voltage standard. The converters with higher measuring ranges are calibrated against the two lower calibrated converters in a setup process (bootstrap). To this end, a parallel connection between the converters and a coaxial T-junction is established, and the converter with the higher voltage range is calibrated against a calibrated converter of the next lower range. The measurement is carried out with the nominal voltage of the calibrated converter, while the second converter is operated at the lower limit of its measuring range.

The transfer difference within the measuring range must remain voltage-independent, in order to avoid additional measurement uncertainties in each of the calibration steps. This applies if neither the resistance value of the range resistor nor the resistance of the heating filament in the thermocouple change within their respective measuring range. This can be checked by means of precise resistance measurements using DC voltage [8]. In order to minimize these measurement uncertainties, thermal converters, whose heating filaments are made of an alloy with a very low temperature coefficient, are used for higher voltages at PTB.

3.3.5 Thermal converters for current measurements

Thermal converters for the quantity RF current are rather unusual, but they are well suited for the use as reference standard in the MHz range. As shown in Figure 3.7, and in contrast to voltage converters, they do not contain a series resistor. Converters with thermocouples for different nominal currents are used for graduated current ranges. The RF current flowing through the converter is measured by way of comparison (identical heating \rightarrow thermoelectric voltage). The current transfer difference δ_i is the characteristic measurement quantity. It is defined in the same way as the voltage transfer difference, but of course in relation to current.

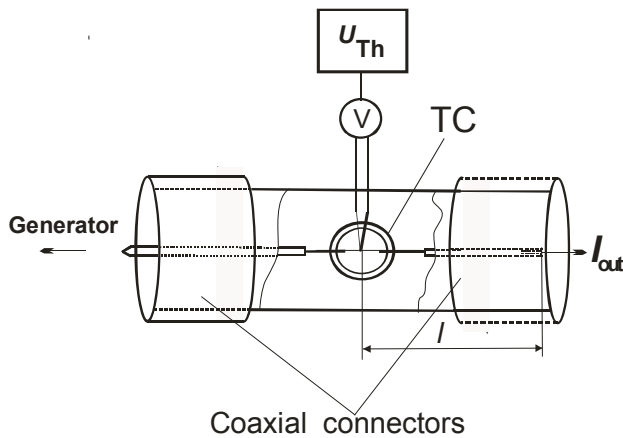


Figure 3.7: Current converter up to 1 GHz

With a sufficiently thin heating filament ($\sim 10 \mu\text{m}$ in diameter for a nominal current of a few mA), the effective resistance of up to nearly 1 GHz no longer depends on the frequency, as can be seen in Figure 3.8.

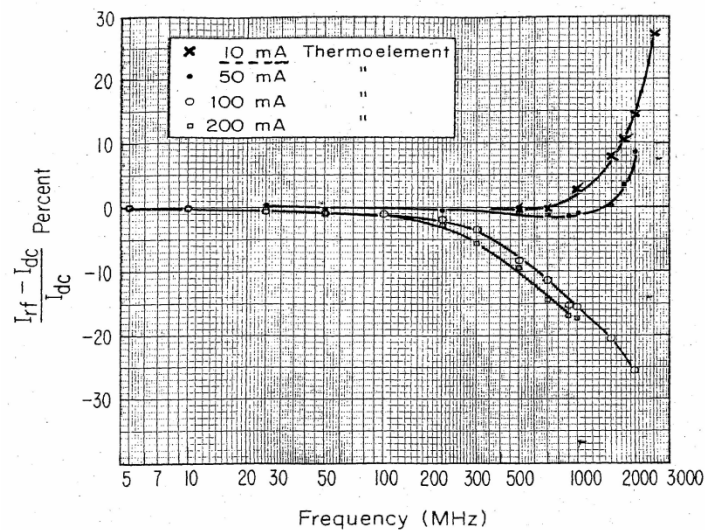


Figure 3.8: Current transfer differences of thermal converters with different nominal currents (Measurement by NBS/NIST in 1968).

Measurement uncertainties arise even at lower frequencies when using thermal converters for current measurement. This can be put down to the divergence between the point of the current measurement at the centre of the transducer and the reference plane at the output of the converter (l in Figure 3.7). As is the case with RF voltage, it is also true for RF current that mismatch at the output port causes a ripple on the supply line inside the converter.

Figure 3.9 shows the measured current transfer differences for two current thermal converters, having different distances (l in Figure 3.8) of 2.3 cm and 3.5 cm between the current measuring plane and the reference plane at the output connector. The measured values are compared to calculated values which result from mismatch between the input impedances of the connected RF current standard and the characteristic impedances in the

current converter. As can be deduced from the good agreement, the measured transfer differences are substantially caused by the **distance between the current measuring planes**. This distance must therefore be kept as small as possible for current converters with low transfer differences.

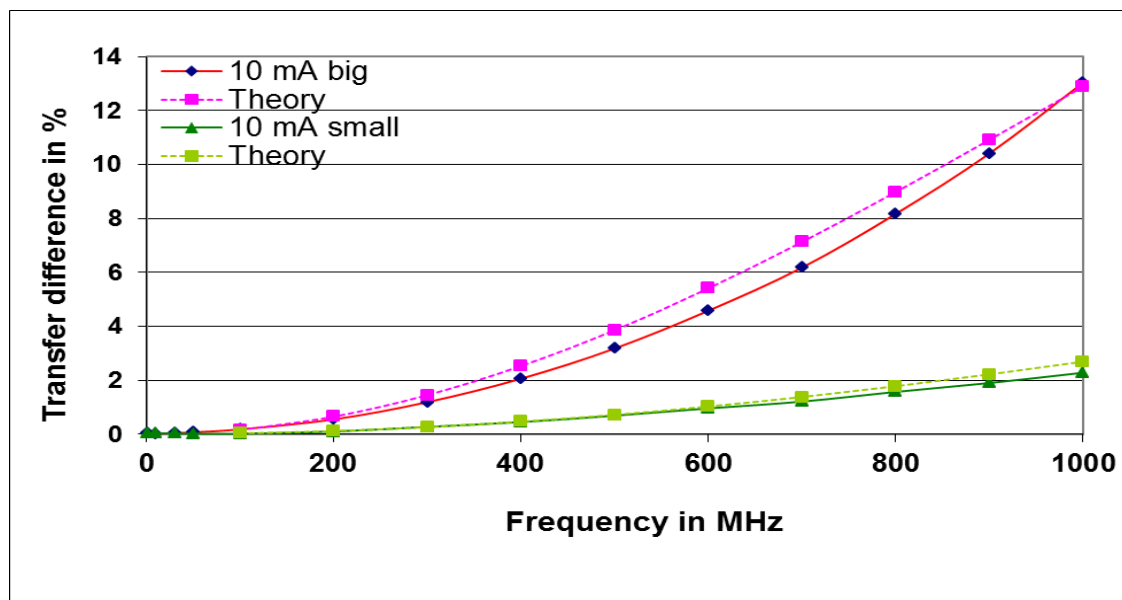


Figure 3.9: Measured current transfer differences for RF current converters with two different lengths $l = 35$ mm (big) and $l = 23$ mm (small) between the measurement plane and the output plane.

3.4 Modelling thermoelectric RF power sensors

The measurement of RF voltage at frequencies above 1 GHz is usually carried out indirectly by way of power measurement, from which the RF voltage is calculated. For this purpose, the frequency-dependent calibration factor and the input impedance of the power meter must be known. Thermoelectric power sensors, which are characterized by a good adaptability, a high degree of linearity and a flat frequency response with regard to their calibration factor, are preferably used as power meters in calibration laboratories. While the determination of the input impedance and the input reflection factor is usually performed by using a network analyzer, the calibration factor is determined by means of a comparison measurement to a power standard.

As shown below, also commercial RF power sensors can be modelled. However, the model is more complex than that of the resistive sensor head (see chapter 4.2). Thus, for example, the input impedance of a thermoelectric sensor head (Rohde & Schwarz NRV-Z51) shows a curve as represented in Figure 3.10.

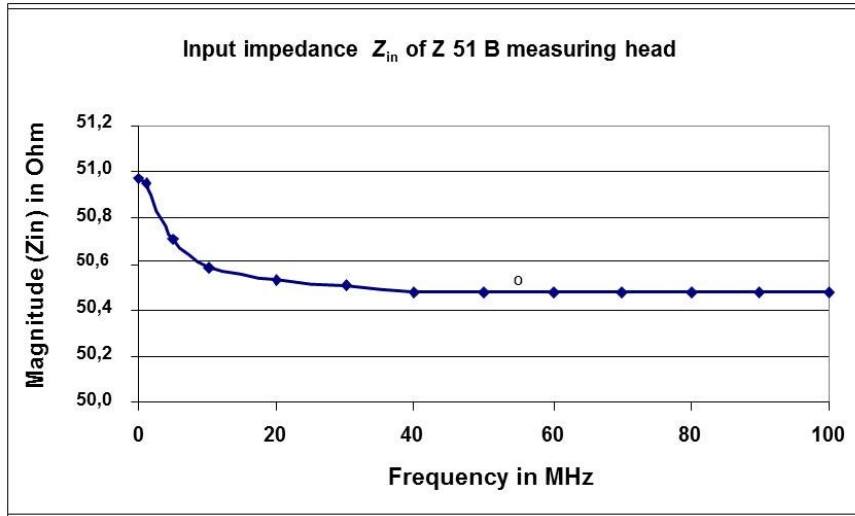


Figure 3.10: Measured value of the real part of the input impedance of a thermoelectric sensor head (type Rohde & Schwarz NRV-Z51).

The manufacturer has confirmed that the increasing course in the lower MHz range is caused by the capacitive coupling of the internal lead of the absorber to the Si-substrate of the sensor element. According to this fact, the sensor model shown in Figure 3.11 can be applied.

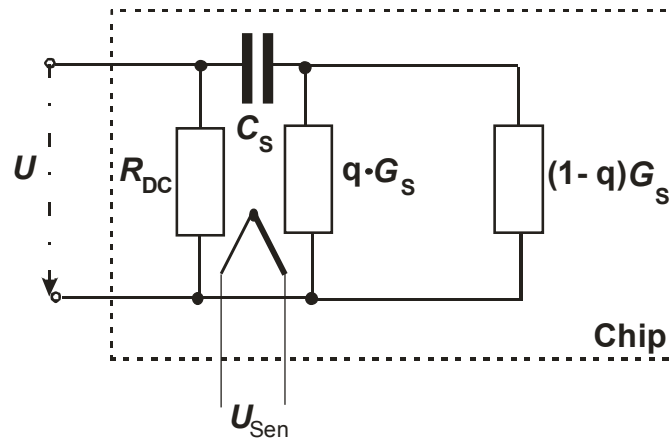


Figure 3.11: Equivalent circuit for the internal set-up of the sensor in the Z51 measuring head.

3.4.1 Equivalent circuit of the sensor

The 50 Ω absorber resistor is indicated as R_{DC} . A thermocouple element is used to measure its heating, which is then indicated on a display unit. Due to the small distance to the Si substrate, a small portion of the RF power is coupled from the coplanar lead to the sensor via the capacitor C_S into the substrate. The substrate is referred to with the conductance G_S .

Input impedance

The value of $R_S = 1/G_S$ results directly from the input impedance at higher frequencies (here 50.5 Ω , R_S parallel R_{DC}). From this, we calculate $R_S = 5400 \Omega$.

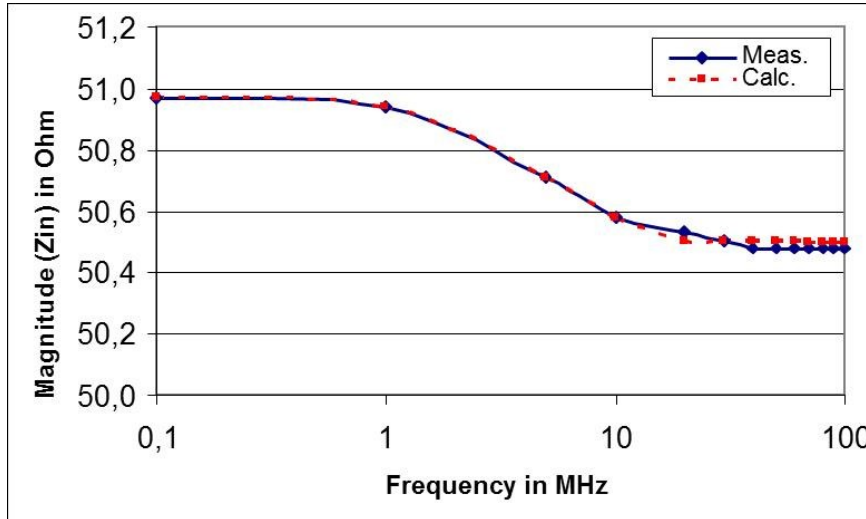


Figure 3.12: Calculated and measured value of the magnitude of the input impedance of the sensor.

If we calculate the value of the real part of the input impedance of R_{DC} and R_S , which according to the equivalent circuit are coupled with one another via C_S , we find a very good agreement between measurement and modeling for $C_S = 6,7 \text{ pF}$. This good agreement confirms the equivalent circuit up to 1 MHz.

Effective efficiency

The conductance $G_S = 1/R_S$ in the equivalent circuit, which takes into account the losses in the substrate, is divided into two parts. On the one hand, we find the proportion $q G_S$, where substrate losses are converted. Since these losses are still fairly close to the thermocouple, they contribute to the temperature indication (U_{TH}). On the other hand, there is the proportion $(1-q) \cdot G_S$, describing the substrate losses which are not detected by the temperature indication. The factor q is initially unknown.

The power loss P_{Loss} , generated by the input voltage U in the substrate resistance $R_S = 1/G_S$, results from the substrate resistance R_P and the current I_P caused by the voltage:

$$R_P = \frac{1}{j\omega C_K} + R_S \quad (3.12)$$

$$I_P = \frac{U}{R_P} \quad (3.13)$$

It follows that:

$$P_P = |I_P|^2 R_S = \frac{U^2}{|R_P|^2} R_S. \quad (3.14)$$

The efficient efficiency η_{eff} for RF power sensors is defined as

$$\eta_{\text{eff}} = \frac{1}{1 + \frac{P_V}{P_{\text{Ind}}}} \quad (3.15)$$

with

$$P_{\text{RF,abs}} = P_{\text{Ind}} + P_{\text{Loss}}. \quad (3.16)$$

Here, P_{Ind} stands for the displayed RF power, $P_{\text{RF,abs}}$ for the entire RF power absorbed by the sensor and P_{Loss} for the proportion of absorbed power that is not displayed.

According to the equivalent circuit,

$$P_{\text{Ind}} = U^2 \cdot (G_{\text{DC}}) + q \cdot P_P \quad (3.17)$$

is obtained for the absorbed RF power.

And for the power loss we obtain

$$P_{\text{Loss}} = (1 - q) \cdot P_P. \quad (3.18)$$

From this we get

$$P_{\text{Ind}} = U^2 \cdot \left(G_{\text{DC}} + q \cdot \frac{R_S}{|R_P|^2} \right) \quad (3.19)$$

and

$$P_{\text{Loss}} = U^2 (1 - q) \cdot \frac{R_S}{|R_P|^2}. \quad (3.20)$$

For the effective efficiency of the sensor, it follows that:

$$\eta_{\text{eff}} = \frac{1}{1 + \frac{P_{\text{Loss}}}{P_{\text{Ind}}}} = \frac{1}{1 + \frac{(1 - q) \frac{R_S}{|R_P|^2}}{G_{\text{DC}} + q \cdot \frac{R_S}{|R_P|^2}}} = \frac{G_{\text{DC}} + q \cdot \frac{R_S}{|R_P|^2}}{G_{\text{DC}} + \frac{R_S}{|R_P|^2}} = \frac{G_{\text{DC}} \cdot |R_P|^2 + q \cdot R_S}{G_{\text{DC}} \cdot |R_P|^2 + R_S}. \quad (3.21)$$

Skin effect losses in the supply line between the connector and the absorber resistor also contribute to the effective efficiency $\eta_{\text{eff,tot}}$ of the complete sensor head. This portion is treated as an adapter with losses connected in series, and taken into account with an effective efficiency according to

$$\eta_{\text{eff,Line}} = \frac{1}{1 + k \cdot \sqrt{f}} \quad (3.22)$$

The effective efficiency of the sensor head is calculated as:

$$\eta_{\text{eff,tot}} = \eta_{\text{eff}} \cdot \eta_{\text{eff,Line}} \quad (3.23)$$

The still unknown values for k and q are obtained by adapting the calculated value to the measurement curve. Thus you obtain, for example $q = 0,45$ und $k = 0,000505$.

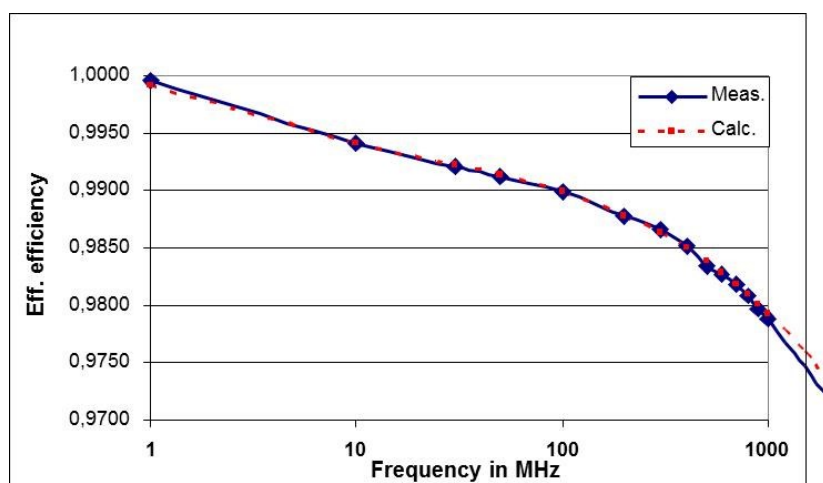


Figure 3.13: Effective efficiency η_{eff} of a NRV-Z51 sensor head over frequency.

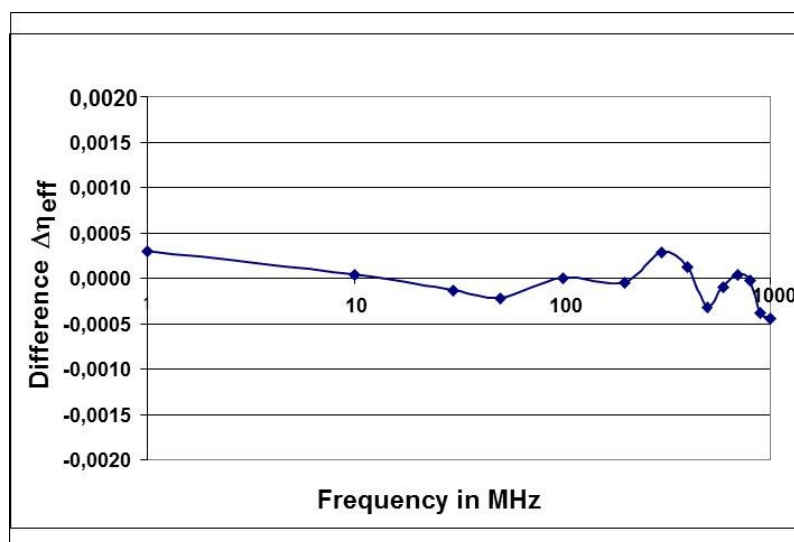


Figure 3.14: Difference of $\Delta\eta_{\text{eff}}$ between measurement and calculation over frequency.

Up to 1000 MHz, the differences $\Delta\eta_{\text{eff}}$ between calculation and measurement lie below 0.0005, and thus below the uncertainties of the measuring values. Due to the smooth course of the measured values below approx. 50 MHz, the calculated correction values of the model can be used for the RF voltage measurement. Thus it is possible to obtain lower uncertainties for the correction values than it would be the case when using the measurement values of the reflection and the calibration factor.

4. Traceability of the measurand RF voltage

At PTB, the measurand RF voltage U_{HF} is traced back to the measurands RF power (calibration factor η_{cal}) and impedance (reflection factor Γ). The RF impedance is traced back to coaxial air lines, i. e. to mechanical dimensions, and the RF power is traced back to the microcalorimeter, i. e. to DC power.

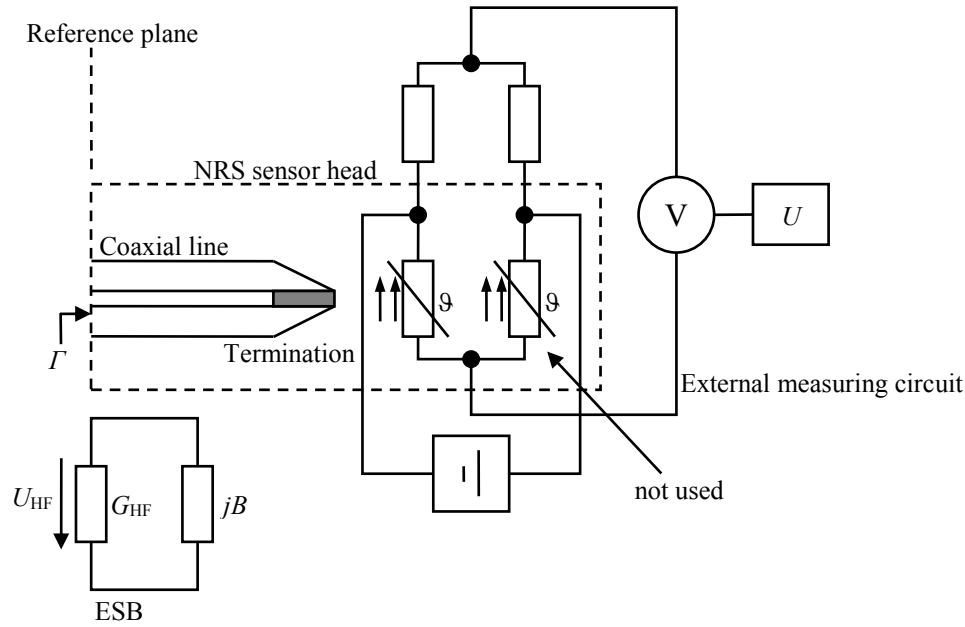


Figure 4.1: RF voltage standard of PTB (R&S NRS sensor head) with DC-coupled absorption power meter and equivalent circuit diagram (EC) for the input.

Figure 4.1 shows the schematic view of a RF voltage standard. The heating of the absorption resistor is detected by means of bridge detuning. The absorbed RF power at the sensor input is

$$P_{\text{RF,abs}} = U_{\text{RF}}^2 G_{\text{RF}}, \quad (4.1)$$

with G_{RF} denoting the conductance of the sensor head input impedance R_{HF} . The following relation is valid between G_{RF} and the input reflection factor of the sensor head Γ (referred to $Z_0 = 50 \Omega$)

$$G_{\text{RF}} = \frac{1}{Z_0} \frac{1 - |\Gamma|^2}{|1 + \Gamma|^2}. \quad (4.2)$$

The substituted DC power P_{DC} , which produces the same display as does P_{RF} , amounts to

$$P_{\text{DC}} = U_{\text{DC}}^2 G_{\text{DC}}. \quad (4.3)$$

The effective efficiency η_{eff} of the resistive sensor head is determined by comparison with a thermistor mount that has been calibrated in the microcalorimeter of PTB:

$$\eta_{\text{eff}} = \frac{P_{\text{DC}}}{P_{\text{ab,RF}}} \Big|_{\text{constant indication}} \quad (4.4)$$

The effective value of the measuring voltage U_{RF} is calculated by comparison with the equivalent DC voltage U_{DC} in the sensor head:

$$U_{\text{RF}} = \sqrt{\frac{1}{\eta_{\text{eff}}} \frac{G_{\text{DC}}}{G_{\text{RF}}}} U_{\text{DC}} \quad (4.5)$$

4.1 Traceability to the measurands reflection factor and calibration factor

Given that

$$\eta_{\text{cal}} = (1 - |\Gamma|^2) \eta_{\text{eff}} \quad (4.6)$$

and using the equation (4.2), it follows that:

$$U_{\text{RF}} = \sqrt{\frac{G_{\text{DC}} Z_0}{\eta_{\text{cal}}}} |1 + \Gamma| U_{\text{DC}} \quad (4.7)$$

and from this it follows that

$$U_{\text{RF}} = \sqrt{\frac{P_{\text{DC}} Z_0}{\eta_{\text{cal}}}} |1 + \Gamma| \quad (4.8)$$

with

$$\eta_{\text{cal}} = \frac{P_{\text{Ind}}}{P_{\text{in}}} \quad (4.9)$$

for RF, and according to the equation


$$\eta_{\text{cal,DC}} = \frac{P_{\text{Ind}}}{P_{\text{DC}}} \quad (4.10)$$

for DC it follows for a constant indication that

$$U_{\text{RF}} = \sqrt{\frac{P_{\text{in}} Z_0}{\eta_{\text{cal,DC}}}} |1 + \Gamma| \quad (4.11)$$

Here, $\eta_{\text{cal,DC}}$ represents a correction of the display with a known DC power. By using the equation (4.3) we obtain the model equation for the RF voltage:

$$U_{\text{RF}} = U_{\text{DC}} \sqrt{\frac{G_{\text{DC}}}{\eta_{\text{cal}} G_0}} |1 + \Gamma| \quad (4.12)$$

	Procedures for a traceable RF voltage measurement https://doi.org/10.7795/550.20190509	DKD-L 02-2	
		Edition:	04/2014
		Revision:	0
		Page:	34 / 47

4.2 Theoretical calculation of the input impedance of the NRS resistive sensor head

In addition to the effective efficiency η_{eff} , the ratio of the DC conductance G_{DC} to the RF conductance G_{RF} at the input port of the sensor head is needed, in order to calculate the voltage measurement error when using a NRS sensor head as RF voltage standard.

The ratio can be determined from RF impedance measurements. At present, however, it is only possible to achieve a measurement uncertainty of approx. 0.3 %. However, impedance measurements with a network analyzer show that, up to 500 MHz, the sensor heads are very well matched and the frequency dependence is very smooth. In the lower MHz range, the differences between the measured values of the impedance and the DC value mostly lie within the defined measurement uncertainty range. To reduce the measurement uncertainty caused by the impedance of the NRS sensor head at low frequencies, the following model is assumed:


The terminating impedance Z_{ab} in the NRS is transformed into the input by a short line of known length in the sensor head (see Figure 4.1). In detail, the procedure will be as follows:

1. The terminating impedance Z_{ab} is modelled as follows: the real part of the resistance R_{E} is set equal to the DC resistance ($R_{\text{E}} = R_{\text{DC}}$), assuming a yet unknown reactance $X = j\omega A$ for the taper around the resistor. A is chosen in such a way as to reach an optimal agreement between the measured values and the model values of the input impedance.
2. It is further assumed that, via the line in the sensor head having the length l (approx. 10.5 cm), the terminating impedance Z_{ab} is transformed with the characteristic impedance Z_{0i} into the input plane. For this purpose, the length l is mechanically measured. For a finer adjustment, it is still possible to slightly change this measured value. In case of the characteristic impedance of the line, the skin effect has to be taken into account, especially at low frequencies. In order to reach an optimal agreement between measurement and model value, the exact value of the characteristic impedance Z_{0i} (approx. 50 Ω) must again be determined by optimization and variation.
3. This model calculation is performed using a PC. In addition, the measured input impedance values Z_{in} are determined, and the measurement and model values are displayed in a diagram. The model parameters are varied until the curves almost overlap in the diagram.
4. Up to about 300 MHz, the model values are used for HF voltage correction and above 300 MHz, the measured values are used.
5. The following approximations are introduced to simplify the calculation:

$$|Z| \cong \frac{1}{|Y|} \quad \text{and} \quad |R| \cong \frac{1}{|G|}. \quad (4.13)$$

Due to the good match of the NRS sensor heads ($R \cong 50 \Omega$ und $X \leq 1 \Omega$), this approximation only causes very slight deviations.

6. The good agreement between model calculation and measurement values for several different NRS sensor heads confirms the reliability of the modeling procedure. Moreover, one example of the sensor head (NRS 3), whose DC resistance had suddenly changed, demonstrates that only R_{DC} has to be changed correspondingly, in order to again obtain a good agreement between model and measurement. In the range below 100 MHz, it is also possible to reach a very good agreement with the measured values by a thermal converter modeled in a different way.

	Procedures for a traceable RF voltage measurement https://doi.org/10.7795/550.20190509	DKD-L 02-2	
		Edition:	04/2014
		Revision:	0
		Page:	35 / 47

4.2.1 Power dependence of the absorption resistor

Due to its small dimensions (approx. 1 mm in diameter), the 50 Ω absorber resistor of carbon in the resistive sensor heads slightly depends on the measurement performance. This can be neglected during power measurement, but not during voltage measurement. When measuring the reflection factor to determine the input impedance, only a very small measurement power is used. The input resistance is measured practically without power. At a voltage of 1 V, for example, the resistor is charged with 20 mW. In doing so, the resistance slightly changes. To be specific, its resistance value decreases by approx. 0.08 Ω / 20 mW. Since the sensor head contains a coaxial line of approximately 11 cm in length between the connector and the resistor, the change in resistance has different effects on the input resistance, dependent on the frequency.

4.3 Determination of the effective efficiency of NRS sensor heads

The effective efficiency η_{eff} of the NRS sensor head is calibrated by means of comparison with two thermistor mounts, which have previously been calibrated in the microcalorimeter. In the lower MHz range, the NRS resistive sensor heads only show small frequency-dependent losses which (within this range) lie below the smallest microcalorimeter measurement uncertainties (approx. 0.2 %). Moreover, highly precise power measurements can only be carried out to a limited extent, due to the bad match of the thermistor mounts and coupling problems below approx. 30 MHz.

In order to exploit the good measurement capabilities of the DC-coupled NRS sensor heads and the small losses in the lower MHz range, the following procedure will be applied:

Above 30 MHz, η_{eff} is determined by means of comparison with a calibrated thermistor mount ($\eta_{\text{eff,Bolo}}$). Assuming that in the NRS resistive sensor head η_{eff} is caused only by the skin effect, a theoretical efficiency $\eta_{\text{eff,Theo}}$ is calculated:

$$\eta_{\text{eff,Theo}} = \frac{1}{1 + C\sqrt{f}} \quad (4.14)$$

Here, $C\sqrt{f}$ is the loss factor, which rises with the square root of the measuring frequency.

By comparing $\eta_{\text{eff,Bolo}}$ and $\eta_{\text{eff,Theo}}$ as well as by adjusting the constant C for an optimal agreement, η_{eff} values with very small measurement uncertainties are obtained for the lower MHz range. The assumed measurement uncertainty for the values obtained by this extrapolation is approximately the deviation between the η_{eff} values and the optimal value 1. This adjustment is carried out for various NRS sensor heads. The different heads show a very similar process with only slight scattering. Besides, values for η_{eff} have been calculated from the know material data for the line inside the head, which are in the low MHz range very close to the measured values.

Furthermore, there exists a replica of the NRS resistive sensor head (ASMW No 4) by the company ROBOTRON. This sensor head has a shorter line of approximately just 9 cm and a conductive layer of pure silver. The **calculated** losses of this ASMW sensor head amount to only 0.2 % at 1 GHz. Loss measurements that were carried out in the same way as for the NRS heads showed an even flatter loss process and a measurement value of approx. 0.27 % at 1 GHz.

The good agreement of the results for two different constructions provides a reliable confirmation of the model. Measurement uncertainties which are **lower** than those of the microcalorimeter measurements can thus be derived by extrapolation in the lower MHz range. Indeed they are based on microcalorimeter measurements, but only at higher frequencies where the losses are greater than the measurement uncertainties of the microcalorimeter.

5. Measurement procedures for RF voltage

In chapter 2.4 we have already dealt with

- the spatially dependent voltage along a line U_x ,
- the incident voltage U_{inc} ,
- the voltage at the reference impedance U_{Z0} .

The established calibration procedures for these measurands will be described in the following sections.

5.1 Measurement by means of a T-junction

Even in the RF range, thermal converters and oscilloscopes with input impedances far above 50Ω are commonly used in the frequency range up to approx. 100 MHz. The calibration of these high-resistance devices requires a clearly defined measurement plane. As is customary in low-frequency technology, these high-resistance measuring instruments are calibrated by parallel connection with a calibrated voltage standard. So here the RF voltage is measured as potential difference between the two conductors, as it is the case in the low frequency range. The calibration voltage at the standard as well as at the measurement object is the voltage in the centre of the T-junction which, in contrast to the power splitter, does not contain any internal resistances. **This means that the voltage is calibrated with regard to the centre of the T-junction.** Unless otherwise mentioned, only commercial coaxial T-junctions, that are compatible with the input connector, are used. Thus, the same T-junction must be used again after calibration. Otherwise, the measurement value will be distorted.

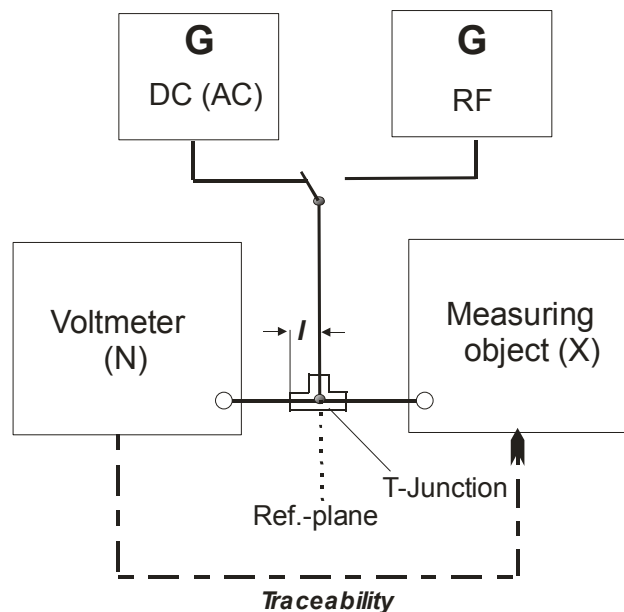


Figure 5.1: Calibration by means of a DC (AC)-RF comparison with T-junction for high-resistance and matched measurement objects.

This measurement procedure is suitable for both high-resistance voltmeters and 50Ω voltmeters, since the generator, in combination with the voltage standard, constitutes a source with a negligibly low internal resistance for the measurement object. If a matched, calibrated RF power meter with a known input impedance voltage and with traceability to power and impedance is used as voltage standard during the measurement according to


	Procedures for a traceable RF voltage measurement https://doi.org/10.7795/550.20190509		DKD-L 02-2	
			Edition:	04/2014
			Revision:	0
			Page:	37 / 47

Figure 5.1, then the voltage with respect to the input level is known. In order to determine or estimate the voltage in the centre of the T-junction, i.e. at a distance l from the input level, the change of voltage caused by the shifting of the reference plane at the centre of the T-piece has to be taken into account (see section 2.5).

When using commercial T-junctions, the standard and the measurement object must have the same connector. At PTB, also self-made T-junctions are used for common coaxial conductor systems, thus allowing the calibration of two devices with different connectors with this procedure.

For the calibration of converters up to 1 GHz (section 3.3.3) with integrated T-junction, the voltage standard is connected directly to the converter by means of the N-connector (female connector). Afterwards, this calibrated converter is used to calibrate the measurement objects in relation to the input level of the N connector of the measurement objects. T-junctions can be avoided by using this special converter, however this implies being dependent on a connector (N connector).

For **high-resistance** voltmeters, this measurement procedure by means of a T-junction is often limited to frequencies up to 100 MHz. Voltmeters with a **matched input impedance**, however, can be calibrated up to approx. 1 GHz by means of a T-junction, since compliance with the reference plane is not necessary.

5.2 Measurement of the incident voltage by means of power splitters

At high frequencies, a precise measurement of the voltage as a potential difference is no longer feasible (see section 2.4). Instead, the amplitude of the incident voltage wave (U_{inc}) is measured. This is a common practice for oscilloscopes with bandwidths far above 1 GHz [9][10]. The determination of the amplitude of the incident voltage U_{inc} is based on a power measurement and a conversion according to:

$$U_{inc} = \sqrt{2P_{inc}Z_0} \quad (5.15)$$

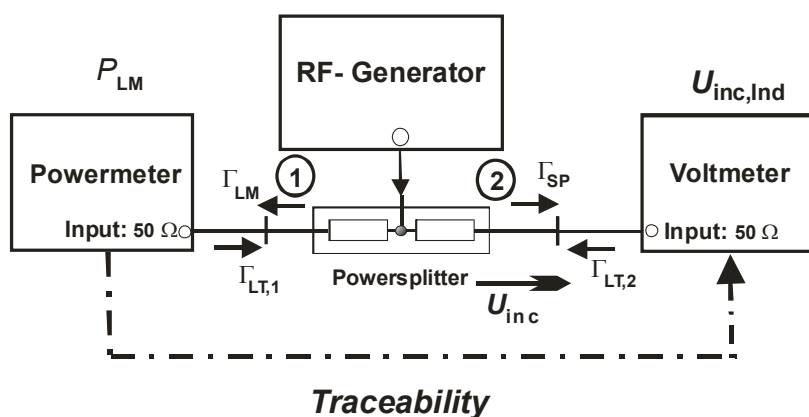



Figure 5.2: Calibration of the incident voltage U_{inc} by means of a power meter.

Assuming a symmetrical resistive power splitter, the incident power $P_{inc,SP}$ on the voltmeter is calculated from the power indication $P_{Ind,LM}$ at the calibrated voltmeter as follows:

$$P_{inc,SP} = \frac{P_{Ind,LM}}{\eta_{cal,LM}} \cdot \frac{|1 + \Gamma_{LT,1}\Gamma_{LM}|^2}{|1 + \Gamma_{LT,2}\Gamma_{SP}|^2} \quad (5.2)$$

	Procedures for a traceable RF voltage measurement https://doi.org/10.7795/550.20190509		DKD-L 02-2	
			Edition:	04/2014
			Revision:	0
			Page:	38 / 47

Here, $\eta_{\text{cal,LM}}$ represents the calibration factor, determined during the calibration of the power meter. By using equation (5.1), we obtain the incident voltage of the measuring device that is to be calibrated:

$$U_{\text{inc,SP}} = \sqrt{\frac{2P_{\text{Ind,LM}} \cdot Z_0}{\eta_{\text{cal,LM}}}} \cdot \frac{|1 + \Gamma_{\text{LT},1} \Gamma_{\text{LM}}|}{|1 + \Gamma_{\text{LT},2} \Gamma_{\text{SP}}|}. \quad (5.3)$$

If all the reflection factors are small, the contribution of U_{inc} to the measurement uncertainty turns out to be very small, due to the products of the reflection factor. The measurement uncertainty of the calibration factor and the power indication contribute with only half their value to the overall measurement uncertainty for U_{inc} . Equation (5.3) requires symmetry of the power distribution. In order to reduce measurement uncertainties caused by asymmetry, the mean value of two measurements should be used. The measurement of U_{inc} can be carried out in all areas where power measurement is possible.

The significance of the incident voltage during transition into the low-frequency and DC range can be derived from equation (2.26): at low frequencies, the source and load reflection factors are small ($\Gamma_G \ll 1$ and $\Gamma_L \ll 1$), so here $U_{\text{inc}} \rightarrow U_{Z_0}$ applies.

If the voltage shall be calibrated at higher frequencies as potential difference U_L for a voltmeter with an input impedance of 50Ω , then it can be determined from the incident voltage. For this purpose, the complex reflection factor Γ_{SP} of the voltmeter has to be determined by a vector network analyzer (VNA). The potential difference then is (see equation (2.20)):

$$U_L = |U_{\text{inc}}| |1 + \Gamma_{\text{SP}}|. \quad (5.4)$$

Here, the measurement uncertainty of U_L depends on the measurement uncertainty of the network analyzer measurement.

5.3 RF voltage calibration of 50Ω generators

When calibrating the output voltage of RF generators, one has to bear in mind that, according to equation (2.26), the voltage U_{inc} depends on the adjustment of the connected load (in this case the connected measuring device) and that it does not represent a generator-specific quantity. The characteristic quantity for the RF output voltage of a generator is the effective value of the voltage U_{Z_0} supplied to an ideal load Z_0 ($\Gamma = 0$) (see section 2.4).

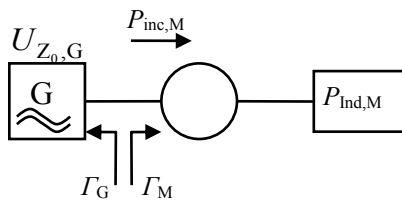



Figure 5.3: Equivalent circuit diagram for RF voltage calibration with 50Ω generators.

	Procedures for a traceable RF voltage measurement https://doi.org/10.7795/550.20190509	DKD-L 02-2	
		Edition:	04/2014
		Revision:	0
		Page:	39 / 47

The measurement of U_{Z_0} is carried out by using a calibrated power meter (M). For this power meter, the following equation applies:

$$P_{\text{inc},M} = \frac{P_{\text{Ind},M}}{\eta_{\text{cal}}}; \quad (5.5)$$

by definition, η_{cal} (also referred to as K_1) indicates the calibration factor of the power meter, while P_{inc} denotes the incident power.

The generator would pass on the power P_{Z_0} to an ideally adapted power meter ($Z_0, \Gamma = 0$).

The incident powers P_{inc} and P_{Z_0} show the following relation

$$P_{Z_0} = P_{\text{inc}} \cdot |1 - \Gamma_G \Gamma_M|^2. \quad (5.6)$$

From this it results that

$$P_{Z_0} = \frac{P_{\text{Ind},M}}{\eta_{\text{cal}}} \cdot |1 - \Gamma_G \Gamma_M|^2. \quad (5.7)$$

The following relationship exists between P_{Z_0} and U_{Z_0}

$$U_{Z_0} = \sqrt{P_{Z_0} \cdot Z_0}, \quad (5.8)$$

so that the equation for the desired voltage becomes:

$$U_{Z_0} = \sqrt{\frac{P_{\text{Ind},M}}{\eta_{\text{cal}}} \cdot Z_0 |1 - \Gamma_G \Gamma_M|^2}. \quad (5.9)$$

Accordingly, it follows

$$U_{\text{inc}} = \sqrt{P_{\text{inc}} \cdot Z_0} \quad (5.10)$$

for the incident voltage

$$U_{\text{inc}} = \frac{U_{Z_0}}{|1 - \Gamma_G \Gamma_M|}. \quad (5.11)$$

Often, only the magnitude of the source impedance [12] of the generator is known. This may lead to measurement uncertainties. However, the resulting measurement uncertainties can be kept relatively small by using a well matched voltmeter.

Oscilloscope calibrators for higher frequencies are to be calibrated for an impedance of 50 Ω as described above: The output voltage U_{Z_0} is to be measured as function of the frequency.

5.4 Generation of low RF voltages

The calibration of very low voltages can be carried out by using the set-up shown in Figure 5.4. For this purpose, one or more attenuators (DGL) are inserted between the output of the power divider and the voltmeter, as is shown in Figure 5.2.

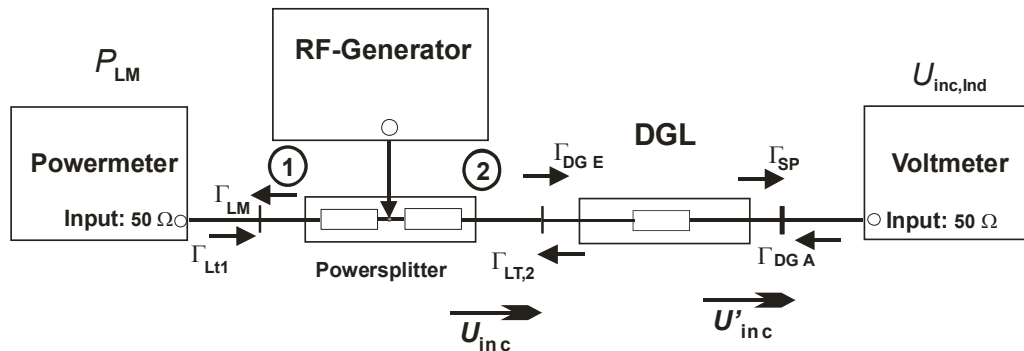


Figure 5.4: Calibration of low incident voltages U_{inc} .

The reduced incident voltage U'_{inc} is calculated as follows:

$$U'_{inc} = \frac{|S_{21DGL}|}{|1 - \Gamma_{DGA} \Gamma_{SP}|} \cdot U_{inc} \quad (5.12)$$

S_{21DGL} represents the insertion loss of the attenuator. Up to 1 GHz, good attenuators have reflection factors of $\Gamma \leq 0,01$. Up to attenuation values of 20 dB, their attenuation can be determined with an uncertainty of 0.003 dB, so the additional uncertainties remain small. Even when cascading several good attenuators, the measurement uncertainty increases only moderately.

6. Calibration of thermal converters as RF voltage transfer standards

6.1 Measuring principle for DC substitution

The calibration of RF thermal converters, which are supplied with a higher-frequency AC voltage, is carried out by determining the AC-DC transfer difference. Metrologically, this quantity is based on the substitution of the **effective value** of the applied RF voltage by an equivalent DC voltage. By heating the filament, the same thermoelectric voltage U_{Th} is thus measured at the thermal converter:

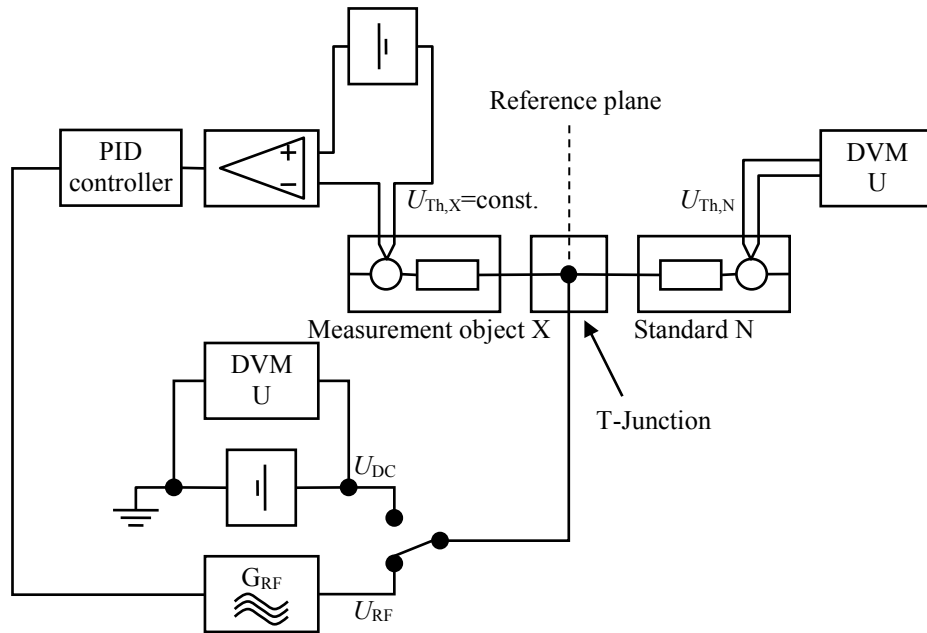


Figure 6.1: Calibration of a thermal converter with DC voltage substitution.

Definition of the **AC-DC transfer difference**:

$$\delta_{DC}(f) = \frac{U_{RF}(f) - U_{DC}}{U_{DC}} \Big|_{U_{Th} = \text{const.}} = \frac{U_{RF}(f)}{U_{DC}} - 1 \Big|_{U_{Th} = \text{const.}} \quad (6.1)$$

Figure 6.1 shows the measurement set-up for a manual converter calibration in which the transfer differences of the measurement object X and a standard N are compared: both converters are fed with a regulated and constant RF voltage U_{RF} , so that the thermoelectric voltage at the measurement object X has the predetermined value $U_{Th,X}$. At the same time, the standard generates the thermoelectric voltage $U_{Th,N}$. Thereafter, the RF voltage is successively replaced by the direct current voltages $U_{DC,X}$ and $U_{DC,N}$ which generate the previously measured voltages $U_{Th,X}$ or $U_{Th,N}$, respectively, at the outputs of the converter.

From the definition of the transfer difference of the standard

$$\delta_{DC,N}(f) = \frac{U_{RF}(f)}{U_{DC,N}} - 1 \Big|_{U_{Th,N} = \text{const.}} \quad (6.2)$$

it follows that

$$U_{RF}(f) = U_{DC,N}(1 + \delta_{DC,N}) \quad (6.3)$$

and, by equating it with the corresponding equation for the measurement object X

$$U_{DC,X}(1 + \delta_{DC,X}) = U_{DC,N}(1 + \delta_{DC,N}) \quad (6.4)$$

the relative transfer difference of the measurement object becomes

$$\delta_{DC,X} = \frac{U_{DC,N}}{U_{DC,X}}(1 + \delta_{DC,N}) - 1. \quad (6.5)$$

The obvious disadvantage of this measuring method is the need to sequentially substitute the thermal voltages in both converters.

6.2 Measuring principle for AC substitution

By substituting the voltage in only one of the converters, namely the measurement object X, and by simultaneously measuring the thermal voltage at the standard, the measurement procedure can be significantly simplified and, above all, automated. At the same time, the substitution is no longer replaced by a DC voltage but by a low-frequency voltage U_{AC} , usually 100 kHz:

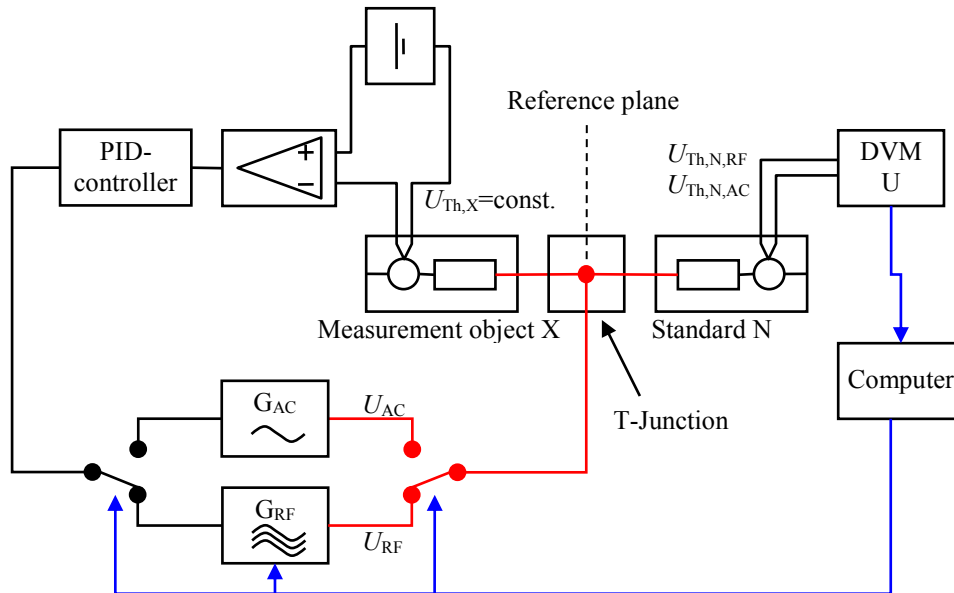


Figure 6.2: Calibration of a thermal converter with AC voltage substitution

For this purpose, a **relative RF-AC transfer difference**

$$\delta_{AC}(f) = \frac{U_{RF}(f)}{U_{AC}(f)} - 1 \Big|_{U_{Th,RF} = U_{Th,AC}} \quad (6.6)$$

is introduced and measured, and then used to calculate the requested relative AC-DC transfer difference $\delta_{DC}(f)$:

$$\begin{aligned}
 \delta_{DC}(f) &= \frac{U_{RF}(f)}{U_{DC}} - 1 = \frac{U_{RF}(f)U_{AC}(f)}{U_{DC}U_{AC}(f)} - 1 \\
 &= \frac{U_{DC}U_{RF}(f) + U_{RF}(f)(U_{AC}(f) - U_{DC})}{U_{DC}U_{AC}(f)} - 1 \\
 &= \frac{U_{RF}(f)}{U_{AC}(f)} + \frac{U_{RF}(f)}{U_{AC}(f)}\delta_{DC}(f_{AC}) - 1 \\
 &= \frac{U_{RF}(f)}{U_{AC}(f)} + \frac{U_{RF}(f)}{U_{AC}(f)}\delta_{DC}(f_{AC}) - 1 + \delta_{DC}(f_{AC}) - \delta_{DC}(f_{AC}) \\
 &= \delta_{DC}(f_{AC})\frac{U_{RF}(f)}{U_{AC}(f) - 1}(1 + \delta_{DC}(f_{AC})) \\
 &= \delta_{DC}(f_{AC}) + \delta_{AC}(f)(1 + \delta_{DC}(f_{AC})), \quad (\delta_{DC}(f_{AC}) \ll 1)
 \end{aligned} \tag{6.7}$$

Here, $\delta_{DC}(f_{AC})$ denotes the AC-DC transfer difference which has been determined by means of an AC/DC transfer measuring station. In the measurement set-up, a control loop stabilizes both the RF and the AC voltage, and synchronizes them in such a way that the thermoelectric voltage $U_{Th,X}$ of the measurement object – according to the definition of the transfer difference – remains constant. From the definition of the relative RF-AC transfer difference according to equation (6.6) it follows for the transfer differences of the measurement object and the standard that

$$\delta_{AC,X}(f) = \frac{U_{RF,X}(f)}{U_{AC,X}(f)} - 1 \Bigg|_{U_{Th,RF,X} = U_{Th,AC,X}} \tag{6.8}$$

and

$$\delta_{AC,N}(f) = \frac{U_{RF,N}(f)}{U_{AC,N}(f)} - 1 \Bigg|_{U_{Th,RF,N} = U_{Th,AC,N}}, \tag{6.9}$$

with the following equations being valid for the measurement process:

$$U_{Th,RF,X} = U_{Th,AC,X} \quad \text{AC substitution in the measurement object X} \tag{6.10}$$

$$U_{RF,X}(f) = U_{RF,N}(f) \quad \text{Parallel connection of measurement object X and standard N} \tag{6.11}$$

$$U_{Th,RF,N} = U'_{Th,AC,N} \neq U_{Th,AC,N} \quad \text{Substitution only in X, but not in N} \tag{6.12}$$

In equation (6.12), $U'_{Th,AC,N}$ represents the thermoelectric voltage at the standard, provided that $U_{AC,X}$ is applied to the measurement object X. The problem is that $U_{AC,N}$ is not substituted in the standard according to the definition in equation (6.9); instead it has to be calculated from $U'_{Th,AC,N}$. Using equation (6.9), the following applies:

$$U_{RF,N}(f) = (1 + \delta_{AC,N}(f))U_{AC,N}(f) \tag{6.13}$$

The insertion of equation (6.11) and equation (6.13) into equation (6.8) yields

$$\delta_{AC,X}(f) = \frac{U_{AC,N}(f)}{U_{AC,X}(f)}(1 + \delta_{AC,N}(f)) - 1. \tag{6.14}$$

The characteristic input and output curve of the standard can be approximated by an exponential function according to the following equation

$$U_{Th} = k(U_{inc})^n \quad (6.15)$$

Here, U_{inc} denotes the RF or AC voltage. Typically, the converter parameter n lies in a range between 1.6 and 2, being a known parameter for the standard.

From equation (6.15) it follows that

$$\left(\frac{U_{AC,1}}{U_{AC,2}}\right)^n = \frac{U_{Th,1}}{U_{Th,2}} \quad (6.16)$$

During calibration, the RF voltage $U_{RF,X} = U_{RF,N}$ in the measurement set-up is substituted by an AC voltage $U_{AC,X}$, so that $U_{Th,X}$ remains constant according to the definition (6.8). **Simultaneously**, the voltage $U'_{Th,AC,N}$ at the standard is measured. This measured voltage, however, is not equal to the voltage $U_{Th,RF,N}$. Figure 6.3 illustrates their relationship. When using the equation (6.15), the valid relation for the quantities at the standard is

$$\left(\frac{U_{AC,N}}{U_{AC,X}}\right)^n = \frac{U_{Th,RF,N}}{U'_{Th,AC,N}} \quad (6.17)$$

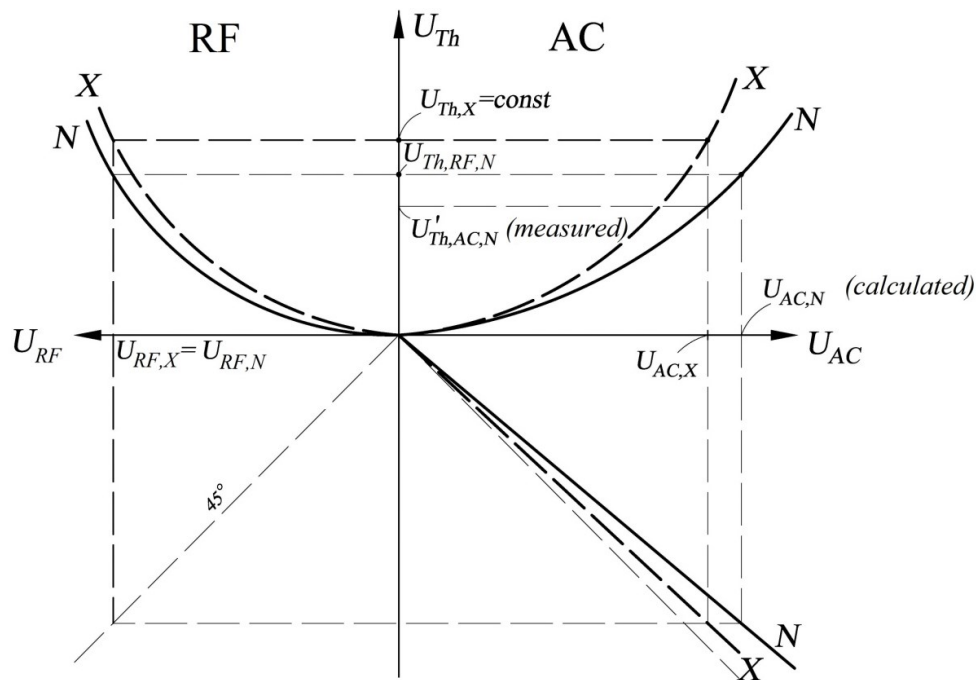



Figure 6.3: Voltages at the characteristic curves of the standard N (solid line) and of the device under test (dashed line).

	Procedures for a traceable RF voltage measurement https://doi.org/10.7795/550.20190509	DKD-L 02-2	
		Edition:	04/2014
		Revision:	0
		Page:	45 / 47

When inserting equation (6.17) into equation (6.14), the following applies for the desired high-frequency AC voltage

$$\delta_{AC,X}(f) = \sqrt[n]{\frac{U_{Th,RF,N}}{U'_{Th,AC,N}}} (1 + \delta_{AC,N}(f)) - 1. \quad (6.18)$$


7. RF voltage calibration of oscilloscopes

The various RF voltage measurement procedures described above are often used for calibrating oscilloscopes and oscilloscope calibrators. The application of the measurement procedures for these devices is specified in the guidelines [10] and [11]. This article may also be seen as a kind of supplement, since it provides a more detailed explanation of the theories regarding the RF voltage measurement procedures. The above-mentioned methods are based on thermal procedures (traceability to power and impedance), which means that the effective value of the RF voltage is measured. In the case of oscilloscopes, however, it is the time dependency of the voltage that is realized, and mainly the peak value \hat{U} of the voltage amplitude that is evaluated. The display of an effective value U_{eff} means that it has been calculated on the assumption of a purely sinusoidal measurement signal according to $\hat{U} = \sqrt{2} \cdot U_{\text{eff}}$. But if the measurement signal for calibration contains harmonics, this relation can lead to deviations. In the worst case, the amplitudes of the fundamental wave \hat{U}_C and those of the harmonic \hat{U}_O can add up to the harmonic peak value $|\hat{U}_S| \leq |\hat{U}_C| + |\hat{U}_O|$. The possible relative measurement deviation $\Delta\hat{U}/\hat{U}$ with $\Delta\hat{U} = \hat{U}_S - \hat{U}_C$ between the peak value \hat{U}_S , biased by a harmonic, and the unbiased peak value \hat{U}_C can be calculated from the harmonic component. It indicates the ratio of the voltage amplitude of the harmonics (O) to the amplitude of the fundamental wave (C) as a logarithmic measure (dBc). Table I shows the possible relative voltage measurement deviations $\Delta\hat{U}/\hat{U}$ for decadic values of the harmonic component.

Table I:

Relationship between the harmonic component inside the generator signal and the possible relative measurement deviations $\Delta\hat{U}/\hat{U}$ when measuring the peak value of the RF voltage

Harmonic component in dBc	Relative measurement deviation $\Delta\hat{U}/\hat{U}$ in %
-10	31.6
-20	10
-30	3.2
-40	1
-50	0.32
-60	0.1

	Procedures for a traceable RF voltage measurement https://doi.org/10.7795/550.20190509	DKD-L 02-2	
		Edition:	04/2014
		Revision:	0
		Page:	46 / 47

8. Bibliography

- [1] Michel, H.-J.: *Zweitor-Analyse mit Leistungswellen*, Stuttgart, B.G. Teubner, 1981.
- [2] Hoffmann, M.: *Hochfrequenztechnik, Ein systemtheoretischer Zugang*, Berlin, Springer, 1997.
- [3] Gustrau, F.: *Hochfrequenztechnik, Grundlagen der mobilen Kommunikation*, München, Hanser, 2013.
- [4] Laiz, H., Klönz, M., et. al.: [New Thin-Film Multijunction Thermal Converters with Negligible Low Frequency AC-DC Transfer Differences](#), IEEE Trans. Instr. Meas., Vol. 50: pp. 333-337, April 2001.
- [5] *Spannungs- und Leistungsmesstechnik, Grundlagen, Begriffe, Produkte*. Company brochure Rohde & Schwarz: www.rohde-schwarz.com/Service&Support.
- [6] Huang, D.-X., et al.: *RF-DC Differences of thermal Voltage Converters Arising from Input Connectors*. IEEE Trans. Instr. Meas., Vol. 40, pp. 360-365 April 1991.
- [7] Free, G.M., et al.: *Characterization of RF- DC Transfer Differences for Thermal Converters With Built-in Tees in the Frequency Range 1 MHz to 1 GHz*. IEEE Trans. Instr. Meas., Vol. 56, pp. 341-345 April 2007.
- [8] Janik, D.: *Über die Spannungsabhängigkeit der relativen Wechselspannungs-Gleichspannungs-Transferdifferenz bei HF-Spannungs-Transfernormalen*, In: H. Bayer (Hrsg.): *Spezielle Entwicklungen und Verfahren der Hochfrequenzmeßtechnik*. PTB-Bericht PTB-E-24, Braunschweig: PTB, December 1983, pp. 131-146.
- [9] Janik, D., et. al.: *Methoden der HF-Spannungsmessung im Vergleich: Anwendung auf die Kalibrierung von Oszilloskopen im GHz-Bereich*, In: H. Bachmair und U. Stumper (Hrsg.): *Aktuelle Probleme der Weitergabe von HF-Meßgrößen*. Vorträge des 139. PTB-Seminars. PTB-Bericht E-58, Braunschweig: PTB, June 1998, pp. 94-111.
- [10] Guideline VDI/VDE/DGQ/DKD 2622 Blatt 4 *Kalibrieren von Messmitteln für elektrische Größen: Oszilloskope*.
- [11] EURAMET Guide cg-7: *Calibration of Measuring Devices for Electrical Quantities: Calibration of Oscilloscopes*, Version 1.0, June 2011, www.euramet.org.
- [12] Reichel, T.: *Messverfahren für den äquivalenten Reflexionsfaktor von HF-Leistungsteilern*, 139. PTB Seminar, 13.5.1998, Braunschweig.
- [13] Török, A., et al.: *Efficient Broadband Method for Equivalent Source Reflection Coefficient Measurements*. IEEE Trans. Instr. Meas., Vol. 50, No. 2, pp. 361 – 363, 2001.



Editor:

Physikalisch-Technische Bundesanstalt
Deutscher Kalibrierdienst
Bundesallee 100
38116 Braunschweig

www.dkd.eu
www.ptb.de